FINITE TIME BLOWUP FOR THE EULER EQUATION

OPENAI

Abstract. We exhibit finite-time blowup for the three-dimensional incompressible, unforced Euler equations from smooth, compactly supported, divergence-free initial data.

Contents

1. Introduction

We study the incompressible Euler equations on $\mathbb{R}^3$:

$$\partial_t u + (u \cdot \nabla)u + \nabla p = 0, \qquad \nabla \cdot u = 0, \qquad u(\cdot, 0) = u_0. \tag{1.1}$$

Here $u(t,x) \in \mathbb{R}^3$ is the velocity and $p(t,x) \in \mathbb{R}$ is the pressure. Spatial norms below are over $\mathbb{R}^3$, unless a different domain is specified. We prove that a smooth initial velocity can develop a singularity in finite time. We take the initial datum in

$$C^\infty_{c,\sigma}(\mathbb{R}^3) = \{u_0 \in C^\infty_c(\mathbb{R}^3; \mathbb{R}^3) : \nabla \cdot u_0 = 0\} \tag{1.2}$$

and write $T_*(u_0)$ for the maximal lifespan of its smooth Euler solution. Local existence gives $T_*(u_0) > 0$ [10].

Theorem 1.1. *There exists $u_0 \in C^\infty_{c,\sigma}(\mathbb{R}^3)$ such that $0 < T_*(u_0) < \infty$. Its smooth Euler solution satisfies*

$$\limsup_{t \uparrow T_*} \|\nabla u(t)\|_{L^\infty} = \infty, \qquad \int_0^{T_*} \|\operatorname{curl} u(t)\|_{L^\infty}\, dt = \infty.$$

1.1. **Historical context.** The Beale–Kato–Majda criterion [1] identifies the time integral of the maximum vorticity as the quantity controlling continuation of a smooth three-dimensional Euler solution. Finite-time breakdown therefore requires this integral to diverge.

Previous singularity constructions depend strongly on the regularity of the initial data and the geometry of the domain. Elgindi [6] proved finite-time blowup on $\mathbb{R}^3$ for axisymmetric velocities without swirl in $C^{1,\alpha}$, for sufficiently small $\alpha > 0$. The stability analysis with Ghoul and Masmoudi [7] gives finite-energy localization. Córdoba, Martínez-Zoroa, and Zheng [5] constructed finite-energy solutions whose initial data are smooth away from one point by coupling separated vorticity regions. More recent preprints of Chen and Shkoller [2, 12] treat finite-energy whole-space velocities without swirl in $C^{1,\alpha}$ for every $0 < \alpha < 1/3$.

For smooth initial data, Chen and Hou [3, 4] proved blowup in an axially periodic cylinder with an impermeable wall, combining analysis with rigorous numerical estimates. The whole-space examples above start below smooth regularity, while this smooth-data construction uses a physical boundary. The setting of Theorem 1.1 combines smooth, compactly supported initial velocity with the boundaryless domain $\mathbb{R}^3$.

Our construction uses the amplification of short waves by a background flow. The instability criteria of Lifschitz and Hameiri and of Friedlander and Vishik [11, 9] describe this mechanism through the evolution of a wavevector and its transverse velocity amplitude. Elgindi and Pasqualotto [8] connected Taylor–Couette instability to singularity formation from $C^{1,\alpha}$ data smooth away from a circle. Here we insert growing, localized oscillations into a sequence of exact smooth Euler solutions. We control their nonlinear effect on the background while making their initial increments summable in every Sobolev norm. The next section explains how this amplification can be repeated on successively shorter time intervals.

2. The amplification mechanism and proof order

Short-wave instability suggests a route to blowup: a small velocity perturbation can develop a large gradient. We seek a flow in which this amplification repeats, with the shear produced by one oscillation amplifying the next over a shorter time interval. To obtain smooth initial data, however, these increasingly large gradients must arise from perturbations whose contributions at time zero are summable in every Sobolev norm. Controlling the pressure is essential to reconciling this initial smallness with the later growth.

2.1. **Flow deformation and wave amplification.** We follow the oscillations in particle coordinates, where their phase remains fixed. A particle starting at a has trajectory $X(t,a)$ given by

$$\partial_t X(t,a) = u(t, X(t,a)), \qquad X(0,a) = a.$$

Along this trajectory, set

$$F = \nabla_a X, \qquad M(t,a) = \nabla u(t, X(t,a)), \qquad H(t,a) = \nabla^2 p(t, X(t,a)). \tag{2.1}$$

Incompressibility gives $\det F = 1$. Differentiating the trajectory equation and $\partial_{tt} X = -\nabla p(t,X)$ gives

$$F_t = MF, \qquad F_{tt} = -HF. \tag{2.2}$$

Thus the pressure Hessian controls the acceleration of the deformation. The corresponding vorticity equation is

$$(\partial_t + u\cdot\nabla)\omega = (\omega\cdot\nabla)u, \qquad \omega = \operatorname{curl} u.$$

Its stretching term describes the change in vorticity along a trajectory. To turn this amplification into a construction, we track both the phase and the velocity of a localized oscillation, which we call a packet.

Write $a = \ell y$, where $\ell > 0$ is the localization length, and choose a unit vector m_0 and a large frequency k. The phase is $k m_0 \cdot y$. Its physical gradient is $(k/\ell)m$, where $m(t,y) = F(t,\ell y)^{-T} m_0$. The principal velocity coefficient $v(t,y)$ satisfies

$$m_t = -M^T m, \qquad v_t = -Mv + 2m\frac{m\cdot Mv}{|m|^2}, \qquad m\cdot v = 0, \tag{2.3}$$

with M evaluated at $(t, \ell y)$. The last term in the velocity equation preserves $m \cdot v = 0$, so v remains orthogonal to the phase normal m. For an amplitude $\alpha > 0$, a nonnegative compactly supported cutoff $\chi_1(y)$, and a smooth periodic profile f_δ with sufficiently small $\delta > 0$, the leading velocity increment is

$$w_{\text{lead}}(t, X(t, \ell y)) = \frac{\ell \alpha}{k} \chi_1(y) v(t, y) f_\delta(k m_0 \cdot y). \tag{2.4}$$

Differentiating the phase produces the leading gradient $\alpha \chi_1 v \otimes m \, f'_\delta$. The small velocity prefactor ℓ / k therefore permits a large gradient.

Along the central trajectory, the parent gradient contains a rank-one shear hqp^T, with scalar amplitude h and orthogonal unit vectors p, q. The shear acts together with the rest of the parent gradient to rotate m and amplify v. At the target time, the directions $m/|m|$ and $v/|v|$ define the normal and transverse velocity of the next frame. Choosing α makes the new leading rank-one gradient the parent shear for the next packet; Proposition 4.1 quantifies both the growth and the transfer of directions.

Nonlinear interactions also produce corrections with zero phase frequency. To separate them, we first regard the phase as an independent variable $\theta \in \mathbb{T} = \mathbb{R}/(2\pi\mathbb{Z})$ and write

$$\langle A \rangle_\theta = \frac{1}{2\pi} \int_0^{2\pi} A(t, y, \theta) \, d\theta. \tag{2.5}$$

The mean is this phase average; the oscillatory part has zero average. The linear boundary value problems in (3.18) and (3.26) determine the two parts, including the spatially nonlocal mean pressure. We then correct the remaining error by an exact evolution and evaluate the resulting fields at $\theta = k m_0 \cdot y$. This evaluation is the restriction to the physical phase graph.

2.2. **Initial smallness and control of pressure.** Repeated amplification gives a candidate singularity only if the initial perturbations still sum to a smooth field. We express these two requirements using exact smooth solutions U^j on nested time intervals and selected times t_j increasing to a finite limit T_∞:

$$|\nabla U^j(t_j, 0)| \longrightarrow \infty, \qquad \sum_j \|U^j(0) - U^{j-1}(0)\|_{H^m} < \infty \quad \text{for every fixed } m. \tag{2.6}$$

The second condition requires control of the packet before its amplification begins. If activation occurs at $t_0 > 0$, we solve a displacement boundary value problem on $[0, t_0]$, with zero displacement at time zero and a prescribed endpoint at t_0. We call this interval the packet's history. The endpoint is chosen to select the growing transverse solution after activation, while the history estimates control the initial velocity increment. At $t_0 = 0$, the transverse velocity is prescribed directly.

These displacement problems rely on a one-sided pressure bound,

$$H \le K_+ I, \quad \text{that is,} \quad \eta^T H \eta \le K_+ |\eta|^2.$$

Together with the initial gradient bounds and the short time interval, it gives coercivity of the displacement form whose interior term is $\int (|\eta_t|^2 - \eta^T H \eta) \, dt$; see (3.11). Large negative eigenvalues of H increase this form. We consequently control the positive eigenvalue contribution of each new packet, using the leading increment

$$\Delta H_{\text{lead}} = -2\alpha \chi_1 (m \cdot Mv) \frac{m \otimes m}{|m|^2} f'_\delta(\theta). \tag{2.7}$$

After a short initial part of the amplification interval, the geometric construction gives $m \cdot Mv > 0$. The profile is chosen with $f'_\delta(0) = \delta^{-1}$ and $f'_\delta \ge -C$. Its large positive derivative produces the desired gradient and a negative semidefinite leading pressure increment; the uniformly bounded negative derivative limits the positive pressure increment. The scale choices make these positive contributions and the errors in (3.14) summable. On the history interval and the short initial part of amplification, the full pressure increments satisfy summable bounds.

All initial data have a common compact support. Together with (2.6), this gives convergence to $u_0 \in C^\infty_{c,\sigma}(\mathbb{R}^3)$. If its Euler solution were smooth past T_∞, stability would compare it with every U^j up to t_j, contradicting the growing gradients. This gives $T_*(u_0) \le T_\infty$.

2.3. **The stages of the proof.** An exact packet can be constructed once suitable growth and propagator bounds for its transverse velocity are available. We prove the packet estimate with these bounds as hypotheses, then establish them from the parent shear. This separates the correction problem from the geometry of amplification; Figure 1 shows how they combine in the iteration.

1. **Construct the mean and oscillatory corrections.** In Section 3, a smooth parent flow supplies the coefficients of two linear inverses. Lemma 3.2 controls their derivatives, hence the expansion in inverse frequency and the cancellation of successive coefficients.
2. **Obtain an exact Euler solution.** Section 3.6 removes the remaining error and restricts the solution to the physical phase graph. Proposition 3.1 collects the resulting gradient, pressure, initial-data, and particle-map estimates used in the iteration.
3. **Prove amplification and transfer of the frame.** Proposition 4.1 supplies the growing transverse solution and propagator bound required by the packet construction. It also shows that the frame at the target time satisfies the geometric conditions for another application.
4. **Choose the scales and iterate.** Sections 5.2, 5.3 and 5.5 choose and verify the amplitudes, frequencies, localization lengths, and time intervals. The seed and inductive step in Sections 5.6 and 5.7 produce the solutions U^j with the bounds in (2.6).
5. **Pass to the limiting initial datum.** Section 6 proves smooth convergence of the initial data, applies Euler stability under the assumption of continuation past T_∞, and proves the divergence assertions in Theorem 1.1: unboundedness of $\|\nabla u(t)\|_\infty$ as $t \uparrow T_*$, and $\int_0^{T_*} \|\operatorname{curl} u(t)\|_\infty \, dt = \infty$.

2.4. **Notation and conventions. Particle labels and components.** We write a for a physical particle label and $y = a/\ell$ for its normalization, where $0 < \ell \le 1$. In §4, the physical label is written a, since $a = B_{pq}(t_0)$ denotes the scalar in (4.4). For a coefficient $b(t,a)$, the normalized coefficient $b_\ell(t,y) = b(t,\ell y)$ satisfies $\partial_y^I b_\ell = \ell^{|I|}(\partial_a^I b)(t,\ell y)$; thus normalization does not increase supremum derivative bounds. A dot on a quantity in particle coordinates denotes differentiation in physical time at a fixed label. Oddness, $u(t,-x) = -u(t,x)$, makes the origin a fixed fluid trajectory. For an orthonormal frame (p,q,n), we write $B_{ij} = i \cdot Bj$ and $v_i = i \cdot v$, for $i,j \in \{p,q,n\}$.

Derivative norms. The packet estimates use $s = 6$ and $\mathbb{T} = \mathbb{R}/(2\pi\mathbb{Z})$ with normalized measure. An *ordered word* I of length n is an ordered sequence of n coordinate derivatives, and ∂^I is their composition. For functions on $\mathbb{R}^3$ or $\mathbb{R}^3 \times \mathbb{T}$, set

$$|f|_n = \sum_{|I|=n} \|\partial^I f\|_{H^s}, \qquad |a|_{n,\infty} = \sum_{|I|=n} \|\partial^I a\|_{W^{s,\infty}}. \tag{2.8}$$

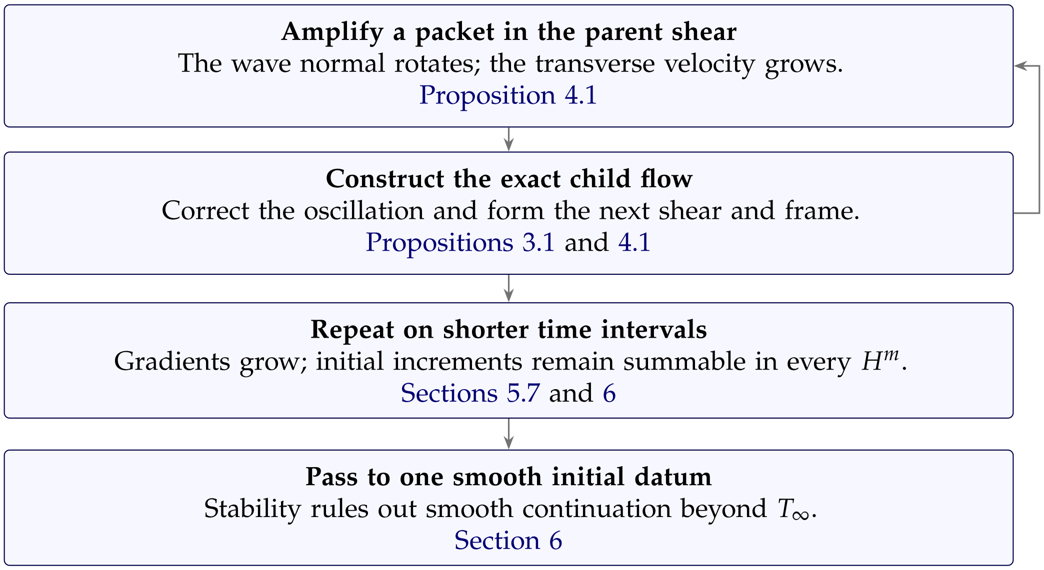

FIGURE 1. One amplification step and its iteration. The child flow supplies the parent shear for the next step. The limiting argument gives $T_*(u_0) \le T_\infty$.

Here a denotes a coefficient, which need not decay at infinity. On a time interval, a norm with a supremum in time means the sum of the supremum for each word; the same word-wise convention applies to L^2 in time. The sum of wordwise suprema is at most d^n times the supremum of the word sum in dimension d, which only changes a fixed growth constant in a factorial estimate.

Gevrey bounds. For the cutoffs and localized expansions, we use Gevrey estimates of order two, $CR^n(n!)^2$. This class contains nonzero smooth compactly supported functions; an analytic estimate has the stronger form $CR^n n!$. Unless stated otherwise, constants in bounds at a fixed derivative order may depend on that order.

Polynomial constants. The parameter $P \ge 2$ collects finitely many coefficient and scale bounds. In the packet estimates, P^c denotes a fixed power that may be enlarged finitely many times. Its exponent may depend on s, the dimension, and the fixed exponent c_0 in the packet data bounds of §3.2, but is independent of the frequency, the number of expansion terms, and the derivative order. In §4, K_h bounds the parent particle map and its first two time derivatives as in (3.15). Powers K_h^c may also be enlarged a fixed finite number of times. Their exponents depend on the fixed low-order bounds, not on the stage or the exponent in the preceding stage's estimate. Constants described as fixed in §5 are independent of the stage index; §5.2 specifies their order of choice.

Notation index. The entries below locate the definitions used in each construction. Symbols attached to a packet or a stage retain the scope of that construction.

Notation	Meaning	Definition
Flow, phase, and primary oscillation		
$C^\infty_{c,\sigma}$, $T_*(u_0)$	Smooth compactly supported divergence-free data on $\mathbb{R}^3$, and the maximal smooth lifespan of the solution from u_0.	(1.2)

Notation	Meaning	Definition
$X,\ F,\ M,\ H$	Particle map, deformation $F = \nabla_a X$, velocity gradient $M = \nabla u$, and pressure Hessian $H = \nabla^2 p$, with the last two evaluated along the parent trajectory.	(2.1)
a, a	Physical particle label; a is used in §4, where a is a scalar coefficient.	§2.4
$\ell,\ y,\ \Xi$	Localization length, rescaled label $a = \ell y$, and $\Xi(t,y) = \ell^{-1}X(t,\ell y)$; also $F = \nabla_y \Xi$.	(3.5)
$\theta,\ \langle\cdot\rangle_\theta$	Independent angle in $\mathbb{T} = \mathbb{R}/(2\pi\mathbb{Z})$, with average $(2\pi)^{-1}\int_0^{2\pi} \cdot\, d\theta$. Physical evaluation uses $\theta = km_0 \cdot y$.	(2.5)
$k,\ \kappa$	Packet frequency in the rescaled label and its inverse $\kappa = k^{-1}$; the physical phase gradient is $(k/\ell)m$.	(3.7)
$m_0,\ m,\ D_m,\ v$	Fixed unit phase normal, transported normal $m = F^{-T}m_0$, $D_m = \|m\|^2$, and primary transverse velocity coefficient $m \cdot v = 0$.	(2.3), (3.7)
$\alpha,\ f_\delta,\ \delta$	Amplitude, odd zero-mean periodic profile, and its concentration parameter; $f'_\delta(0) = \delta^{-1}$. The leading velocity is $(\ell\alpha/k)\chi_1 v f_\delta$.	(2.4), (3.4)
$d_i,\ \widetilde{d}_i,\ D_i$	$d_i = \sum_j (F^{-1})_{ji}\partial_{y_j}$, $\widetilde{d}_i = d_i + km_i\partial_\theta$, and $D_i = \kappa\partial_{y_i} + (m_0)_i\partial_\theta$. Physical graph derivatives are $\ell^{-1}\widetilde{d}_i$.	(3.7); (3.45)
Norms and packet corrections		
$s,\ I,\ \|f\|_n,\ \|a\|_{n,\infty}$	$s = 6$; I is an ordered derivative word. Sum $\\|\partial^I f\\|_{H^s}$, respectively $\\|\partial^I a\\|_{W^{s,\infty}}$, over $\|I\| = n$, on $\mathbb{R}^3$ or $\mathbb{R}^3 \times \mathbb{T}$ as specified.	(2.8)
$P,\ P^c,\ P_j$	Data-size bound $P \geq 2$, fixed polynomial losses, and the bound chosen at stage j. The exponent c in P^c is independent of frequency, expansion length, and derivative order.	§2.4; (5.10)
$R,\ d,\ h(t)$ in shift bounds	Derivative growth constant, nonnegative integer shift, and positive time profile in the factorial bound $R^{n+d}((n+d)!)^2$. This h is a general profile.	(3.1)
$\rho,\ \\|f\\|_\rho$	Radius and weighted derivative norm $\sum_{n\geq 0} \rho^n \|f\|_n/(n!)^2$.	(3.42)
$\chi_1,\ \chi_o$	Fixed even cutoffs: $\operatorname{supp}\chi_1 \subset \{\|y\| < 1/2\}$, $\chi_1(0) = 1$; $\chi_o = 1$ on $\|y\| \leq 1$, supported in $\|y\| \leq 2$.	§3.1
$R_\perp,\ K,\ G,\ K_R$	Orthonormal basis matrix for $m_0^\perp$, $K = F^T F$, $G = K^{-1}$, and $K_R = R_\perp^T K R_\perp$.	(3.10)
$K_h,\ g(t)$	Parent particle-map factorial bound K_h, including its first two time derivatives; positive profile $g(t_0) = 1$ weighting the transverse propagator on $\|y\| \leq 1/2$ by $g(t)/g(s')$, $t_0 \leq s' \leq t \leq S$.	(3.15); §3.2 (iii)
$K_+,\ B_e,\ B_c,\ L$	Upper pressure-Hessian bound $H \leq K_+ I$, lower initial symmetric gradient bounds $-B_e I$ for $\|\ell y\| \geq r$ and $-B_c I$ for $\|\ell y\| < r$, and coefficient L of the initial boundary operator.	(3.11)
$\mathcal{N},\ \mathcal{A}$	Newton operator $(-\Delta_y)^{-1}$ and initial-support operator $\operatorname{curl}_y \chi\mathcal{N}\chi \operatorname{curl}_y$, where $\chi(y) = \chi_o(\ell y)$.	(3.19)

Notation	Meaning	Definition
$A_p,\ B_p,\ Q_p,\ C_p$	Zero-angle-mean transverse and angle-independent velocity coefficients at inverse-frequency order p; vector potential $Q_p = -\partial_\theta^{-1}(m \times A_p)/D_m$ and curl remainder $C_p = d \times Q_p$. The angle primitive has zero mean.	(3.32)
$N_k,\ W^a,\ q^a$	Expansion length $N_k = \lfloor k^\vartheta \rfloor$, $\vartheta = 10^{-6}$, and approximate normalized velocity and pressure increments; physical increments carry factors ℓ and ℓ^2.	(3.33)
Amplification geometry		
$p,\ q,\ n,\ B_{ij}$	Orthonormal frame of an older flow: normalized ray, normalized transverse velocity, and $n = p \times q$; $B_{ij} = i \cdot Bj$ for $i, j \in \{p, q, n\}$.	(4.2)
$B,\ h,\ h_*,\ E$	Older central gradient, current shear amplitude, its activation value, and error in $M(t, 0) = B + hqp^T + E$, with $h(t_0) = h_*$.	(4.3)
$a,\ \beta,\ \varepsilon$	Frozen coefficients $a = B_{pq}(t_0)$, $\beta = B_{nq}(t_0)/a$, and $\varepsilon = \sqrt{a/h_*}$. The physical label in this section is a.	(4.4)
$\tau,\ x,\ x_{\text{prev}},\ x_{\text{tar}}$	Rescaled times $\tau = a(t - t_0)/\varepsilon$, $x = \sqrt{\beta}\,\tau$, previous scale parameter, and target value of x. Here x is not spatial position.	(4.4)
$p_2,\ q_2,\ n_2,\ A_{\text{tar}}$	Child frame $p_2 = m/\lvert m\rvert$, $q_2 = v/\lvert v\rvert$, $n_2 = p_2 \times q_2$, and central target magnitude $A_{\text{tar}} = \lvert m(t_{\text{tar}}, 0)\rvert \lvert v(t_{\text{tar}}, 0)\rvert$.	Proposition 4.1
Iteration and limiting datum		
$U^j,\ p_j,\ M_j,\ H_j$	Exact stage solution and its pressure, with $M_j = \nabla U^j$, $H_j = \nabla^2 p_j$. At stage $j \geq J$, the parent is U^{j-1} and the older solution is U^{j-2}; $U^{J-2} = U_B$ is the base.	§5, §5.4
$x_j,\ h_j,\ k_j,\ \ell_j,\ \delta_j,\ \alpha_j$	Stage scale parameter, target shear, frequency, localization length, profile concentration, and amplitude $\alpha_j = \delta_j h_j / (\lvert m(t_j, 0)\rvert \lvert v(t_j, 0)\rvert)$ for $j \geq J$.	(5.6), (5.18)
$t_j,\ S_j,\ W_j$	Target time, retained horizon, and available width. Stage $j \geq J$ activates at $t_0 = t_{j-1}$, with $t_{J-1} = 0$, and retains $S_j = t_j + 2W_{j+1}$.	(5.7), (5.8)
T_∞	Finite accumulation time $\lim_j t_j$; the limiting datum satisfies $T_*(u_0) \leq T_\infty$.	(6.4), (6.6)

3. A localized oscillation over a smooth Euler flow

We construct an exact Euler solution u^{new} over a smooth parent u, using the leading oscillation (2.4). The prescribed gradient and pressure-Hessian increments are (3.13) and (3.14) in Claim 1 of Proposition 3.1. Compact support of the initial increment is enforced by the mean boundary condition (3.24) and the support-preserving transverse inverse in Lemma 3.2.

We construct the truncated expansion (W^a, q^a) in (3.33) with θ independent of y. Restricting to $\theta = km_0 \cdot y$ introduces a factor of k when the phase is differentiated. Before this restriction, the transport field b^a in (3.41) is small by (3.43). Lemma 3.3 removes the residual (3.44) on $\mathbb{R}^3 \times \mathbb{T}$ and constructs the physical solution (3.46)–(3.47) under the frequency condition (3.12).

3.1. **Norms, cutoffs, and factorial estimates.** We first fix the derivative bounds and cutoff functions used to control all orders of the oscillatory expansion with one growth constant. We use the derivative norms $|f|_n$ and $|a|_{n,\infty}$ of §2.4, which sum the H^6 and $W^{6,\infty}$ norms over ordered derivative words. The data bound $P \geq 2$ and fixed powers P^c follow the conventions in the same section. For $R \geq 1$ and an integer $d \geq 0$, we say that a function has *shift d* with profile $h(t) > 0$ if

$$\sum_{|I|=n} \sup_t h(t)^{-1} \|\partial^I f(t)\|_{H^s} \leq R^{n+d}((n+d)!)^2 \qquad (n \geq 0). \tag{3.1}$$

The same expression with wordwise L^2 time norms will be used in the linear estimates. Here R is the constant controlling derivative growth: a larger R gives a weaker bound. Later we sum these derivatives with weights involving a small radius ρ, chosen proportional to R^{-1}. These are factorial derivative bounds of order two; no analyticity in space is asserted.

Here are the two elementary rules used to keep one growth constant for the entire construction. The Sobolev product inequality in dimension at most four and Leibniz's rule show that the product of shifts d_1, d_2 has shift $d_1 + d_2$, up to a fixed constant, because

$$\frac{\binom{n}{l}((l+d_1)!)^2((n-l+d_2)!)^2}{((n+d_1+d_2)!)^2} = \frac{\binom{n}{l}}{\binom{n+d_1+d_2}{l+d_1}^2} \leq \binom{n}{l}^{-1}, \qquad \sum_{l=0}^{n} \binom{n}{l}^{-1} \leq 3. \tag{3.2}$$

The same proof applies to multiplication $W^{s,\infty} \times H^s \to H^s$. One derivative costs one shift. A coefficient bounded by $P^c R_c^n (n!)^2$, with $R_c = P^c$, can be included at the cost of one additional shift when R is a sufficiently large fixed power of P.

The second rule concerns a triangular estimate

$$Z_n \leq P^c \left(F_n + \sum_{l=1}^{n} \binom{n}{l} R_c^l (l!)^2 Z_{n-l} \right). \tag{3.3}$$

If F_n has shift $d-1$, induction gives shift d for Z_n. Indeed, division by $R^{n+d}((n+d)!)^2$ bounds the data term by P^c/R and the remaining sum by $P^c \sum_{l \geq 1} (R_c/R)^l$ times the largest previous normalized bound. We choose R so that their sum is at most one. This choice depends on the estimate at the fixed Sobolev index producing (3.3), and never on the expansion length.

We fix even smooth cutoffs χ_1, χ_o on $\mathbb{R}^3_y$ with

$$0 \leq \chi_1 \leq 1, \quad \operatorname{supp} \chi_1 \subset \{|y| < 1/2\}, \quad \chi_1(0) = 1,$$
$$\chi_o = 1 \text{ on } \{|y| \leq 1\}, \quad \operatorname{supp} \chi_o \subset \{|y| \leq 2\},$$

and derivative bounds $C^{n+1}(n!)^2$. Such cutoffs follow, for example, from the extension by zero of $\exp(-1/z)$ for $z > 0$. Cauchy's estimate on the complex circle of radius $z/2$ gives $n!(2/z)^n \exp(-c/z) \leq C^{n+1}(n!)^2$; integration, products, and fixed rescalings give the asserted cutoffs. For sufficiently small $\delta > 0$, we also fix a smooth odd periodic function f_δ of mean zero such that

$$f_\delta'(0) = \delta^{-1}, \qquad -C \leq f_\delta' \leq \delta^{-1}, \qquad \|\partial_\theta^n f_\delta\|_{H^{s+2}(\mathbb{T})} \leq \delta^{-c}(C\delta^{-c})^n (n!)^2. \tag{3.4}$$

To see this explicitly, take an even nonnegative bump $g \leq 1$ supported in a small subinterval of $(-\pi, \pi)$, with $g(0) = 1$, and put $c_g = \langle \delta^{-1} g(\theta/\delta) \rangle_\theta$. This number is independent of δ. The even function

$$h_\delta(\theta) = \frac{\delta^{-1} g(\theta/\delta) - c_g}{1 - c_g \delta}$$

has mean zero, maximum δ^{-1} at zero, and a uniform lower bound. Its odd periodic primitive is f_δ. The derivative estimates follow from the cutoff estimates and the bounded mean-zero integration operator.

3.2. **Coordinates and hypotheses.** We write the velocity increment as $\ell W(t,y,\theta)$ in the particle coordinates $x = X(t,\ell y)$, where X is the parent particle map, ℓ is the localization length, and y is the rescaled particle label. The angle $\theta \in \mathbb{T}$ is initially an independent variable. To obtain the physical increment we restrict to $\theta = km_0 \cdot y$, where k is the frequency and m_0 is a fixed unit phase normal. The coefficient and propagation assumptions below are the inputs to Proposition 3.1.

Let u be a smooth odd Euler velocity on $[0,S]$, where $0 < S \le 1$, with pressure p, and let $X(t,a)$ be its particle map:

$$X_t(t,a) = u(t,X(t,a)), \qquad X(0,a) = a.$$

The map $X(t,\cdot)$ preserves volume and $X(t,0) = 0$. Fix $0 < \ell \le 1$ and define

$$\Xi(t,y) = \ell^{-1}X(t,\ell y), \quad F = \nabla_y \Xi, \quad M = (\nabla u)(t,X(t,\ell y)), \quad H = (\nabla^2 p)(t,X(t,\ell y)). \tag{3.5}$$

Differentiation of the particle equation and of Euler's equation gives

$$\det F = 1, \qquad F(0) = I, \qquad F_t = MF, \qquad F_{tt} = -HF. \tag{3.6}$$

Set $d_i = \sum_j (F^{-1})_{ji}\partial_{y_j}$. These are the commuting derivatives in the coordinates Ξ; the Jacobian identity gives $d \cdot W = \operatorname{div}_y(F^{-1}W)$.

Fix a constant unit vector m_0 and a frequency $k > 0$, and put

$$m = F^{-T}m_0, \qquad D_m = |m|^2, \qquad \widetilde{d} = d + km\partial_\theta, \qquad \kappa = k^{-1}. \tag{3.7}$$

We first regard θ as an independent periodic variable. The *graph restriction* of a function $a(t,y,\theta)$ is $a(t,y,km_0 \cdot y)$. Its derivative in the normalized physical coordinates $\Xi = x/\ell$ is $\widetilde{d}a$; the physical derivative is $\ell^{-1}\widetilde{d}a$. In particular the components of $\widetilde{d}$ commute. Adding the physical velocity ℓW and pressure $\ell^2 q$, evaluated on this graph at $x = X(t,\ell y)$, preserves Euler's equation exactly when

$$W_t + MW + W \cdot \widetilde{d}W + \widetilde{d}q = 0, \qquad \widetilde{d} \cdot W = 0. \tag{3.8}$$

Fix $t_0 \in [0,S)$ and a constant 3×2 matrix $R_\perp$ whose columns are an orthonormal basis of $m_0^\perp$. Also fix $\alpha > 0$. The time t_0 separates the history interval $[0,t_0]$, when $t_0 > 0$, from forward evolution on $[t_0,S]$. We first prescribe the primary velocity coefficient v. If $t_0 > 0$, choose a constant $\xi_T \in \mathbb{R}^2$ with $|\xi_T| \le P^{c_0}$ and let $\eta = FR_\perp \xi$, with $\xi(0) = 0$ and $\xi(t_0) = \xi_T$, be stationary for

$$\int_0^{t_0} (|\eta_t|^2 - H\eta \cdot \eta)\, dt.$$

Set $v = FR_\perp \xi_t$ on this interval. If $t_0 = 0$, prescribe $v(0)$ to be a constant unit vector in $m_0^\perp$. In either case, continue v from t_0 by

$$v_t = -Mv + 2m\frac{m \cdot Mv}{D_m}. \tag{3.9}$$

The stationary displacement exists uniquely under the coercivity condition below, as proved in the transverse inverse construction. Thus v is constructed from the prescribed endpoint or initial data; its existence on the history interval is not an additional assumption.

The matrices used in the inverse estimates are

$$K = F^TF, \qquad G = K^{-1} = F^{-1}F^{-T}, \qquad K_R = R_\perp^T K R_\perp. \tag{3.10}$$

The following assumptions concern these coefficients, the time interval, and the forward propagation of the primary equation.

(i) **Coefficient and scale bounds.** The coefficients $F, F^{-1}, F_t, F_{tt}, M, H$ have multiplier bounds $P^{c_0}(P^{c_0})^n(n!)^2$. The matrices K, G, K_R have eigenvalues bounded below by P^{-c_0}, and the scalar D_m satisfies $D_m \geq P^{-c_0}$. Their inverses have the same type of multiplier bounds. The inverses of S and, when positive, t_0 are at most P^{c_0}. Also $\ell^{-1}, \delta^{-1} \leq P^{c_0}$.

(ii) **Quadratic-form bounds and coercivity.** For nonnegative K_+, B_e, B_c, the quadratic-form bounds

$$H \leq K_+ I, \qquad \operatorname{sym} M(0) \geq -B_e I \quad \text{if } |\ell y| \geq r, \qquad \operatorname{sym} M(0) \geq -B_c I \quad \text{if } |\ell y| < r$$

hold, where $0 < r < 1/4$. With the dimensional constants C_1, C_2 in (3.22), assume

$$\frac{K_+ S^2}{2} + B_e S + C_2 B_c r^3 S \leq \frac{1}{2}, \qquad L \geq C_1 B_c, \qquad 0 \leq L \leq P^{c_0}. \tag{3.11}$$

If the bound with B_e holds everywhere, we may take $B_c = 0$.

(iii) **Transverse propagation and amplitude.** At each fixed label $|y| \leq 1/2$, write a solution of the homogeneous equation (3.9) as $A = FR_\perp a$. For $t_0 \leq s' \leq t \leq S$, its transverse propagator, the linear solution map $a(s') \mapsto a(t)$, has operator norm at most $P^{c_0} g(t)/g(s')$, where $g > 0$ and $g(t_0) = 1$. The amplitude satisfies $\alpha, \sup_{[t_0,S]} \alpha g \leq P^{c_0}$.

All the data are smooth.

For the packet estimate, fix the hypothesis exponent c_0 and let u be a smooth odd Euler velocity on $\mathbb{R}^3 \times [0, S]$, $0 < S \leq 1$, with pressure p and particle map X. Take $P \geq 2$ and $0 < \ell \leq 1$, and define F, M, H by (3.5). Use the even spatial cutoffs χ_1, χ_o fixed in §3.1 and the smooth odd mean-zero periodic profile f_δ satisfying (3.4). Fix a unit phase normal $m_0 \in \mathbb{R}^3$, frequency $k > 0$, activation time $t_0 \in [0, S)$, and amplitude $\alpha > 0$, and set $m = F^{-T} m_0$. Let v be the transverse velocity coefficient prescribed in §3.2. For $t_0 > 0$, choose a constant orthonormal basis matrix $R_\perp$ for $m_0^\perp$ and endpoint $\xi_T \in \mathbb{R}^2$ with $|\xi_T| \leq P^{c_0}$. Set $v = FR_\perp \xi_t$, where $FR_\perp \xi$ is the stationary displacement with $\xi(0) = 0$ and $\xi(t_0) = \xi_T$. For $t_0 = 0$, take $v(0)$ to be a constant unit vector in $m_0^\perp$. In both cases it evolves after t_0 by (3.9). Assume all data are smooth and satisfy the coefficient, inverse, time, and scale bounds in §3.2 (i), the quadratic-form and coercivity conditions in §3.2 (ii), and the propagator and amplitude bounds in §3.2 (iii).

Proposition 3.1. *There is a finite exponent $Q = Q(c_0)$, uniform over the smooth packet data satisfying §3.2 (i)–(iii), such that for every $k \geq k_0(c_0)$ satisfying*

$$P^Q \leq k^{\vartheta/100}, \qquad \vartheta = 10^{-6}, \tag{3.12}$$

there is a smooth odd exact Euler solution u^{new} on $[0, S]$, with pressure p^{new}.

1. **Gradient and pressure increments.** *At $x = X(t, \ell y)$, with $\theta = k m_0 \cdot y$, its increments satisfy*

$$\nabla u^{\text{new}} - \nabla u = \alpha \chi_1 v \otimes m \, f_\delta'(\theta) + O(k^{-1/4}), \tag{3.13}$$

$$\nabla^2 p^{\text{new}} - \nabla^2 p = -2\alpha \chi_1 (m \cdot Mv) \frac{m \otimes m}{D_m} f_\delta'(\theta) + O(k^{-1/4}). \tag{3.14}$$

The errors are uniform globally in space and on $[0, S]$.

2. **Particle-map bounds.** *Suppose in addition that the parent particle map obeys*

$$\sum_{|I|=n} \sup_{0 \leq t \leq S} \|\partial_a^I (X - \mathrm{id}, X_t, X_{tt})\|_{H^s} \leq K_h^{n+1} (n!)^2, \qquad 1 \leq K_h \leq P^{c_0}. \tag{3.15}$$

Then the particle map X^{new} of u^{new} obeys

$$\sum_{|I|=n} \sup_{0\le t\le S} \|\partial_a^I(X^{\text{new}} - \mathrm{id}, X_t^{\text{new}}, X_{tt}^{\text{new}})\|_{H^s} \le (k^{C_*})^{n+1}(n!)^2, \qquad C_* = 10(s+2). \tag{3.16}$$

3. **Initial increment.** *The initial increment splits as $u_{\text{high},0} + u_{\text{mean},0}$, with supports in $\{|a| \le \ell/2\}$ and $\{|a| \le 2\}$, respectively. For each fixed integer $m \ge 0$,*

$$\|u_{\text{high},0}\|_{H^m} \le \ell^{-m}\alpha k^m P^{c_m}, \qquad \|u_{\text{mean},0}\|_{H^m} \le \ell^{-m}k^{-2}P^{c_m}. \tag{3.17}$$

At a stage with $t_0 = 0$ and $L = 0$, all forced oscillatory coefficients and all mean coefficients have zero initial value; only the prescribed primary oscillation and its curl correction contribute to the initial velocity.

Proof strategy for Proposition 3.1. Compact support at time zero is the first constraint. The mean correction can spread through the nonlocal pressure, so we impose its initial support through a boundary condition on the displacement. Together with the transverse inverse, this gives the corrections needed to reduce the Euler residual to a size that can be removed by exact evolution.

3.3. **A linear inverse with compactly supported initial velocity.** To construct the mean part of the packet in Proposition 3.1, let $f(t,y)$ be an angle-independent forcing. We seek an angle-independent velocity B and pressure $\bar{q}$ satisfying

$$B_t + MB + d\bar{q} = f, \qquad d\cdot B = 0, \qquad \operatorname{supp} B(0) \subset \{|\ell y| \le 2\}. \tag{3.18}$$

Only the initial velocity must have compact support: the pressure and the mean velocity at positive times may be nonlocal. To impose the initial condition, we write a displacement as $\eta = Fz$, with $\operatorname{div}_y z = 0$ and $z(S) = 0$, and recover the velocity as $B = Fz_t$. A boundary operator in the variational equation will force $z_t(0)$ to have the required support. Introduce the Newton operator $\mathcal{N} = (-\Delta_y)^{-1}$, the cutoff $\chi(y) = \chi_o(\ell y)$, and the nonnegative operator

$$\mathcal{A} = \operatorname{curl}_y \chi\mathcal{N}\chi \operatorname{curl}_y. \tag{3.19}$$

Its output is divergence free and supported in $\{|\ell y| \le 2\}$. On the Hilbert space

$$\mathcal{V} = \{z \in H^1((0,S); L^2_\sigma(\mathbb{R}^3)) : z(S) = 0\}, \qquad \|z\|_{\mathcal{V}} = \|z_t\|_{L^2_t L^2_y},$$

where L^2_σ denotes distributionally divergence-free fields, consider

$$a(z,b) = \int_0^S \int_{\mathbb{R}^3} \big((Fz)_t\cdot(Fb)_t - HFz\cdot Fb\big)\,dy\,dt + \langle M(0)z(0), b(0)\rangle + L\langle \mathcal{A}z(0), b(0)\rangle,$$

$$a(z,b) = -\int_0^S \langle f, Fb\rangle\,dt \qquad (b \in \mathcal{V}). \tag{3.20}$$

We first verify boundedness of the boundary operator and then coercivity. For any multiplier ψ,

$$\|\psi \operatorname{curl} z\|_{\dot{H}^{-1}} \le C\big(\|\psi\|_\infty + \|\nabla\psi\|_3\big)\|z\|_2. \tag{3.21}$$

Indeed, pairing with φ and integrating by parts gives $\langle z, \psi \operatorname{curl}\varphi + \nabla\psi\times\varphi\rangle$. Hölder's inequality and $\|\varphi\|_6 \le C\|\nabla\varphi\|_2$ prove (3.21). Applying this inequality to each factor in the Newton pairing bounds $\operatorname{curl}\psi\mathcal{N}\psi' \operatorname{curl}$ on L^2. For our cutoff,

$$\|\partial^I\chi\|_\infty + \|\nabla\partial^I\chi\|_3 \le C^{n+1}(n!)^2 \qquad (|I| = n).$$

Here the factor ℓ^{n+1} in the second term is multiplied by the L^3 scaling factor ℓ^{-1}. Differentiated commutators of $\mathcal{A}$ split the derivatives between its two cutoffs. The same argument, followed by the fixed s derivatives, proves their factorial operator bounds on H^s.

Put $Z = \|\mathcal{N}^{1/2}\chi \operatorname{curl} z(0)\|_2$ and $w = \mathcal{N}\operatorname{curl}(\chi \operatorname{curl} z(0))$. The Fourier multiplier of $\mathcal{N}^{1/2}\operatorname{curl}$ has norm at most one, so $\|w\|_2 \le Z$. Since $-\Delta z(0) = \operatorname{curl}\operatorname{curl} z(0)$, the difference $z(0) - w$ is harmonic on $|y| < \ell^{-1}$. The interior mean-value estimate on its half-ball therefore gives

$$\sup_{|y|<(2\ell)^{-1}} |z(0) - w|^2 \le C\ell^3 \|z(0) - w\|^2_{L^2(|y|<\ell^{-1})}.$$

Multiplying by the volume of $\{|y| < r/\ell\}$ and using $r < 1/4$ yields dimensional constants C_1, C_2 such that

$$\|z(0)\|^2_{L^2(|\ell y|<r)} \le C_1 Z^2 + C_2 r^3 \|z(0)\|_2^2. \tag{3.22}$$

Let $E = \int_0^S \|(Fz)_t\|_2^2\, dt$. Terminal integration gives

$$\int_0^S \|Fz\|_2^2\, dt \le \frac{S^2}{2}E, \qquad \|z(0)\|_2^2 \le SE,$$

where we used $F(0) = I$. Consequently

$$a(z,z) \ge \left(1 - \frac{K_+ S^2}{2} - B_e S - C_2 B_c r^3 S\right) E + (L - C_1 B_c) Z^2 \ge \frac{1}{2}E.$$

Moreover $z_t = F^{-1}(Fz)_t - F^{-1}F_t z$ and terminal integration imply $\|z_t\|^2_{L^2_t L^2} \le P^c E$. Thus the bounded bilinear form is coercive on $\mathcal{V}$, whether or not $M(0)$ is symmetric. The Lax–Milgram theorem gives a unique solution of (3.20).

For completeness, we recover its strong equation and its initial trace. Let $\mathbb{P}_\sigma$ be the L^2 orthogonal projection onto the divergence-free fields L^2_σ. Testing with compact support in time first gives

$$\left(\mathbb{P}_\sigma F^T F z_t\right)_t = \mathbb{P}_\sigma\left[F^T f + ((F^T F)_t - 2F^T F_t) z_t\right].$$

The terms containing z cancel because $F_{tt} = -HF$. On L^2_σ, the operator $T(t) = \mathbb{P}_\sigma F^T F$ is positive with inverse norm P^c. The identity $T(t)^{-1} - T(s)^{-1} = T(t)^{-1}(T(s) - T(t))T(s)^{-1}$ shows that its inverse is continuously differentiable in time. It follows that $z_t \in H^1_t L^2$, and

$$\mathbb{P}_\sigma(F^T F z_{tt}) = \mathbb{P}_\sigma(F^T f - 2F^T F_t z_t). \tag{3.23}$$

We can now integrate (3.20) by parts. At $t = 0$, the term $-M(0)z(0)$ from $-(Fz)_t(0)$ cancels its displayed boundary term, leaving

$$z_t(0) = L\mathcal{A}z(0). \tag{3.24}$$

Both sides are divergence-free in y, so there is no remaining projection in this identity. Set

$$B = F z_t, \qquad d\bar{q} = f - B_t - MB. \tag{3.25}$$

Equation (3.23) says precisely that $F^T(f - B_t - MB)$ is a gradient. Thus $\bar{q}$ exists as a distributional potential, its displayed gradient is in L^2, and $d \cdot B = \operatorname{div}_y z_t = 0$. Finally $B(0) = L\mathcal{A}z(0)$ has the required compact support. Only the initial mean velocity is localized; the mean field at positive times is allowed to be nonlocal.

3.4. **The transverse inverse and its derivative bounds.** With $m = F^{-T}m_0$ and $R_\perp$ as in §3.2, we now construct a velocity coefficient A satisfying $m \cdot A = 0$ and its pressure coefficient π for forcing with zero angle mean. When $t_0 > 0$, a displacement problem determines A on the history interval; a first-order equation governs A for $t \geq t_0$.

For $t_0 > 0$ and a forcing f of zero angle mean, take $\eta = FR_\perp\xi$ with $\xi(0) = \xi(t_0) = 0$, and solve

$$\int_0^{t_0} (\eta_t \cdot \zeta_t - H\eta \cdot \zeta)\,dt = -\int_0^{t_0} f \cdot \zeta\,dt, \qquad \zeta = FR_\perp b, \quad b(0) = b(t_0) = 0. \tag{3.26}$$

This is an equation at each (y, θ); no spatial differentiation occurs. Its coercivity follows from $K_+t_0^2/2 \leq 1/2$. Nonzero terminal data are handled by subtracting $t\xi_T/t_0$ before applying this inverse. The same integration by parts gives, with $K_R = R_\perp^T F^T F R_\perp$,

$$K_R\xi_{tt} = R_\perp^T F^T(f - 2F_tR_\perp\xi_t), \qquad A = FR_\perp\xi_t. \tag{3.27}$$

The matrix K_R defined above is positive. The inverse preserves both spatial support and zero angle mean.

Since $m \cdot A = 0$ and $m_t = -M^Tm$, we have $m \cdot A_t = m \cdot MA$. Thus (3.27) is equivalently

$$A_t + MA + m\partial_\theta\pi = f, \qquad \pi = \partial_\theta^{-1}\left(\frac{m \cdot f - 2m \cdot MA}{D_m}\right). \tag{3.28}$$

Here ∂_θ^{-1} is defined on zero-mean functions by $\widehat{\partial_\theta^{-1}h}(j) = (ij)^{-1}\widehat{h}(j)$ for $j \neq 0$, with zero coefficient at $j = 0$. After t_0 we solve this first-order equation from the value furnished by the history interval. At $t_0 = 0$, forced coefficients use zero initial value. In coordinates $A = FR_\perp a$ the equation is

$$K_Ra_t + 2R_\perp^T F^T F_t R_\perp a = R_\perp^T F^T f. \tag{3.29}$$

The following estimate collects the inverses (3.18) and (3.28), with the shift bounds defined in (3.1). Its transverse conclusion also includes the potential coefficient and curl remainder that will impose exact incompressibility. The integer shift index d is distinct from the differential operator in $d\bar{q}$ and $d\pi$.

Let u be a smooth odd Euler velocity on $\mathbb{R}^3 \times [0, S]$, $0 < S \leq 1$, with pressure p and particle map X. Take $P \geq 2$ and $0 < \ell \leq 1$, and define F, M, H by (3.5). Fix a unit phase normal $m_0 \in \mathbb{R}^3$, frequency $k > 0$, and activation time $t_0 \in [0, S)$. Set $m = F^{-T}m_0$, and let the columns of the constant 3×2 matrix $R_\perp$ form an orthonormal basis of $m_0^\perp$, as in §3.2. Assume all data are smooth, the coefficient, inverse, time, and scale bounds in §3.2 (i), the quadratic-form and coercivity conditions in §3.2 (ii), and the propagator and amplitude bounds with profile g in §3.2 (iii). Use the cutoff χ_o fixed in §3.1 and the shift convention (3.1).

Lemma 3.2. *For the mean inverse (3.20) and transverse inverse (3.28), with smooth data satisfying §3.2 (i)–(iii), there exists a choice $R = P^c$ with the following properties for every integer $d \geq 10$ and every $h_0 > 0$.*

- *(a)* **Mean inverse.** *An angle-independent smooth force f of shift $d - 10$ with constant profile h_0 gives, through (3.20), the fields $B, B_t, d\bar{q}$ of shift d with the same profile, where $B, d\bar{q}$ are defined by (3.25). These fields satisfy (3.18); the initial trace is $B(0) = L\mathcal{A}z(0)$.*
- *(b)* **Transverse inverse.** *Let a smooth force f have zero angle mean and spatial support in $|y| \leq 1/2$. Use zero displacement at both ends of the history interval when $t_0 > 0$, and zero initial velocity when $t_0 = 0$, followed by (3.29). Write A, π for the resulting velocity and pressure*

coefficients in (3.28). Suppose the force has shift $d-10$, separately on these intervals, with profile

$$h(t) = \begin{cases} h_0, & 0 \le t \le t_0, \\ h_0 g(t), & t_0 \le t \le S. \end{cases}$$

Define the vector-potential coefficient Q_A and its curl correction C_A by

$$Q_A = -\partial_\theta^{-1} \frac{m \times A}{D_m}, \qquad C_A = d \times Q_A.$$

Then $A, A_t, \pi, Q_A, C_A, C_{A,t}, d\pi$ have shift d with profile h. The solution is transverse, $m \cdot A = 0$, and these fields retain zero angle mean. Any fixed closed spatial set containing the support of the force at every time also contains the support of these fields.

The choice of R is independent of the shift and the number of expansion terms. Nonzero displacement endpoint data are treated by the affine extension described above.

Proof. We first obtain the estimates at the fixed Sobolev order s, then control additional derivatives by (3.3). Time traces and the forward propagator give the stated time suprema. For the mean form, allow the general right side

$$\int_0^S (\langle g_1, b_t \rangle + \langle g_0, b \rangle)\, dt + \langle g_b, b(0) \rangle.$$

Coercivity, terminal integration, and the trace bound yield

$$\|z_t\|_{L_t^2 L^2} \le P^c(\|g_1\|_{L_t^2 L^2} + \|g_0\|_{L_t^2 L^2} + \|g_b\|_2).$$

Spatial difference quotients preserve L^2_σ and the terminal condition. Subtracting the translated form puts every coefficient difference on the right side. At derivative level j, those terms contain coefficient derivatives in $W^{j,\infty}$ and previously controlled derivatives of z_t of order at most $j-1$. The boundary commutators are controlled by (3.21) with derivatives split between its two cutoffs. Applying the preceding estimate and then taking a weak limit of difference quotients gives the estimate at level j. The finite induction $j = 0, \dots, s$ costs only P^c.

Apply this fixed-s estimate after a word of n additional derivatives. Every commutator puts at least one of those n derivatives on a coefficient. Thus, for the wordwise time norms, it gives exactly (3.3). The coefficient F^T multiplying the forcing can either be included in the top factor P^c or charged one shift using (3.2). Finite higher regularity is first obtained by the same difference-quotient argument, so this sharpened recurrence does not presume existence of derivatives.

The positive inverse $T(t)^{-1}$ in (3.23) has the same estimates at Sobolev order s and after additional derivatives: the projection commutes with derivatives and the L^2 coercivity starts the induction. We obtain z_{tt} in $L_t^2 H^s$, then use the Hilbert-space trace inequality

$$\sup_t \|w(t)\| \le C\big(S^{-1/2}\|w\|_{L_t^2} + S^{1/2}\|w_t\|_{L_t^2}\big) \tag{3.30}$$

for z_t. A further use of the strong equation gives a time supremum for z_{tt} when f is bounded in time. Continuity follows from the strong equation and the continuous inverse. This also justifies all higher-order initial traces. The transverse history inverse has the identical proof with a matrix in place of the projected inverse and with no boundary operator; angle differences are included. An affine extension of endpoint data contributes only general weak data of the form just estimated.

For the forward transverse equation, divide suprema by $g(t)$. Duhamel's formula and the assumed propagator bound give

$$\sup_{t_0\le t\le S}\frac{\|a(t)\|_2}{g(t)}\le P^c\left(\|a(t_0)\|_2+\int_{t_0}^{S}\frac{\|f(t)\|_2}{g(t)}\,dt\right).$$

Differentiating the equation through the fixed s indices puts a derivative of its coefficient matrix against a previously controlled lower derivative of a. There are only s such steps. Words of additional derivatives then give (3.3) with the profile g. All terms remain supported where the propagator estimate is assumed. In particular we never use a Gronwall factor exponential in the undifferentiated matrix norm.

The inverse coefficient bounds used here also follow directly from the original bounds and the polynomial lower eigenvalue bound. Differentiate the identity $AA^{-1}=I$ through the fixed $W^{s,\infty}$ indices. A word of additional derivatives gives a triangular convolution with at least one derivative on A, and the same absorption proves its factorial bounds after increasing a fixed power of P.

To make the derivative accounting explicit, an input force of shift $d-10$ gives successively the following available shifts:

$$\begin{array}{c|ccccc} \text{quantity} & z_t \text{ in } L^2_t & z_{tt} \text{ in } L^2_t & z_t \text{ in } L^\infty_t & z_{tt} \text{ in } L^\infty_t & B, B_t, d\bar{q} \\ \hline \text{shift} & d-9 & d-8 & d-7 & d-6 & \le d-4. \end{array} \tag{3.31}$$

Each inverse uses (3.3); products and the time trace use the rules already proved. For the transverse inverse the history calculation is the same. At t_0, its forward data $a(t_0)=\xi_t(t_0)$ have shift $d-7$. The forward inverse gives $d-6$, multiplication to obtain A costs one shift, and (3.28) gives A_t with at most one more. Hence π, Q_A have shift at most $d-4$, $Q_{A,t}$ at most $d-3$, $C_A, d\pi$ at most $d-2$, and $C_{A,t}$ at most $d-1$. One final shift covers the sum of the two time intervals. The support, mean, and transverse properties follow from the inverse constructions and the formulas for Q_A, C_A. □

3.5. **Cancelling the coefficients of the oscillatory expansion.** We expand the normalized velocity W and pressure q in (3.8) in powers of $\kappa=k^{-1}$. The quadratic term can have nonzero angle mean even when the leading oscillation has zero mean, so cancelling the residual requires both mean and oscillatory corrections. Lemma 3.2 supplies these corrections with the required support and growth bounds. At each order, the mean equation can be solved before the oscillatory equation, giving the recursion below.

Let $N_k=\lfloor k^{\vartheta}\rfloor$. The index p below denotes a power of κ, not a derivative order. We seek zero-mean transverse fields A_p and angle-independent fields B_p satisfying $m\cdot A_p=0$ and $d\cdot B_p=0$. Define their vector potentials and the associated curl remainders by

$$Q_p=-\partial_\theta^{-1}\frac{m\times A_p}{D_m},\qquad C_p=d\times Q_p,\qquad V_p=A_p+B_p+C_{p-1},\quad C_0=0. \tag{3.32}$$

The role of C_p is exact incompressibility. Indeed $m\times\partial_\theta Q_p=A_p$, so

$$\kappa^p A_p+\kappa^{p+1}C_p=\kappa^{p+1}\widetilde{d}\times Q_p.$$

The approximation is

$$W^a=\sum_{p=1}^{N_k}\big(\kappa^p(A_p+B_p)+\kappa^{p+1}C_p\big),\qquad q^a=\sum_{p=1}^{N_k}\big(\kappa^p\bar{q}_p+\kappa^{p+1}\pi_p\big), \tag{3.33}$$

and $\widetilde{d} \cdot W^a = 0$ identically. We set $B_1 = 0$, $\bar{q}_1 = 0$, and $A_1 = \alpha\chi_1 v f_\delta$. Before t_0, multiplication of the primary displacement by $\alpha\chi_1 f_\delta$ produces this same velocity coefficient, because its equation contains no spatial derivatives.

Here is the precise coefficient extraction. Extend the notation by $V_{N_k+1} = C_{N_k}$ and $V_p = 0$ outside $1 \le p \le N_k + 1$. The coefficient of κ^p in the quadratic term with label derivatives is $\sum_{i+j=p} V_i \cdot dV_j$; in the term with a phase derivative it is $\sum_{i+j=p+1}(V_i \cdot m)\partial_\theta V_j$. Thus for $2 \le p \le N_k$ the forcing for $A_p + B_p$ is

$$f_p = -C_{p-1,t} - MC_{p-1} - d\pi_{p-1} - \sum_{i+j=p} V_i \cdot dV_j - \sum_{i+j=p+1} (V_i \cdot m)\partial_\theta V_j. \tag{3.34}$$

There is no phase-derivative term of order zero, since the positive indices i, j cannot satisfy $i + j = 1$. The term of order one vanishes because $V_1 = A_1$ and $m \cdot A_1 = 0$. In (3.34), the only undetermined nonzero term is $-(B_p \cdot m)\partial_\theta A_1$. Separate it by writing

$$f_p = f_p^{\text{known}} - (B_p \cdot m)\partial_\theta A_1, \qquad \bar{f}_p = \langle f_p^{\text{known}} \rangle_\theta. \tag{3.35}$$

Here f_p^{known} depends only on coefficients already constructed, and $\langle h \rangle_\theta = (2\pi)^{-1} \int_0^{2\pi} h \, d\theta$. The undetermined term has zero angle mean. We first solve

$$B_{p,t} + MB_p + d\bar{q}_p = \bar{f}_p, \qquad d \cdot B_p = 0, \tag{3.36}$$

using (3.20), with terminal displacement zero and initial trace (3.24). With this B_p fixed, we solve

$$\begin{gathered} A_{p,t} + MA_p + m\partial_\theta \pi_p = f_p^{\text{known}} - \bar{f}_p - (B_p \cdot m)\partial_\theta A_1, \\ m \cdot A_p = 0. \end{gathered} \tag{3.37}$$

using the transverse inverse. Its history displacement has zero values at $0, t_0$ when $t_0 > 0$; at $t_0 = 0$ the forced coefficient has zero initial value. Forward continuation is given by (3.29). Thus each order is constructed from the preceding orders, with the mean solved before the oscillation.

Pure means cannot produce a nonzero angle-dependent term. All oscillatory coefficients, including their curl remainders, are therefore supported in $|y| \le 1/2$. At t_0 the history and forward transverse solutions have the same value and satisfy the same first-order equation. Their first derivatives agree there; induction in time derivatives proves smooth matching. The mean strong equation gives the same time regularity as its forcing. Thus all coefficients are smooth. The oddness of u makes F, M, H even in y. Under $(y, \theta) \mapsto (-y, -\theta)$, both d and ∂_θ reverse parity. Uniqueness of the linear inverses then proves inductively that A_p, B_p, C_p are odd and $Q_p, \pi_p, \bar{q}_p$ are even, the latter pressure being defined up to a constant.

We next prove bounds uniform in N_k. Set

$$\begin{gathered} a_p = 100p - 80 \quad (p \ge 1), \qquad b_p = 100p - 140 \quad (p \ge 2), \\ \gamma(t) = \begin{cases} \alpha, & t \le t_0, \\ \alpha g(t), & t \ge t_0, \end{cases} \qquad H_0 = \max(1, \alpha, \sup \alpha g). \end{gathered} \tag{3.38}$$

With one fixed $R = P^c$, the fields

$$A_p, A_{p,t}, \pi_p, Q_p, C_p, C_{p,t}, d\pi_p$$

have shift a_p and profile γH_0^{2p-2}; the fields $B_p, B_{p,t}, d\bar{q}_p$ have shift b_p and constant profile H_0^{2p-2}.

The shift costs of the two inverses are given in Lemma 3.2 and (3.31). The primary endpoint data $\alpha\chi_1 f_\delta \xi_T$ have polynomial factorial bounds after division by α. The affine extension and these linear estimates use fewer than $a_1 = 20$ shifts. The $t_0 = 0$ primary has the same conclusion from its polynomial initial data.

For the induction in p, the following table displays the largest shift of each forcing term, including its indicated derivative and coefficient multiplications:

forcing term at order p	largest shift	possible output
$V_i \cdot dV_j, i+j=p$	$100p-158$	mean or oscillatory
$(B_i \cdot m)\partial_\theta A_j,\ i+j=p+1$	$100p-118$	oscillatory
$(B_i \cdot m)\partial_\theta C_{j-1},\ i+j=p+1$	$\leq 100p-118$	oscillatory
$(C_{i-1} \cdot m)\partial_\theta (A_j + C_{j-1}),\ i+j=p+1$	$\leq 100p-158$	mean or oscillatory
$C_{p-1,t},\ MC_{p-1},\ d\pi_{p-1}$	$\leq 100p-178$	oscillatory.

For example, the first line uses $a_i + a_j = 100p - 160$; the second uses $b_i + a_j = 100p - 120$. Terms with $A_i \cdot m$ vanish, and pure mean terms have smaller shifts. The target force shifts are $b_p - 10 = 100p - 150$ and $a_p - 10 = 100p - 90$, so all entries have room to spare, including the term involving the newly solved B_p.

The profiles obey the same triangular ordering. A product $V_i \cdot dV_j$ has at most H_0^{2p-2} in a mean equation and retains a factor γH_0^{2p-2} in an oscillatory equation. A phase-derivative product $(B_i \cdot m)\partial_\theta A_j$ has exactly γH_0^{2p-2}. Replacing B_i by C_{i-1} lowers the constant exponent by two, which absorbs any additional factor $\gamma \leq H_0$. Angle averaging and subtraction of the average are bounded operations. There are only $O(p)$ products. To absorb that factor, promote each product first to one below its target shift. The remaining shift contributes $R(n + d_{\text{target}})^2$, with $d_{\text{target}} \geq 25p$, which dominates Cp and every fixed polynomial constant after the single choice of R. The inverse absorption in (3.3) is independent of p. This proves all claimed coefficient bounds with a growth constant independent of the expansion order.

The coefficients are now constructed and bounded at one fixed value of R. It remains to show that truncating the expansion leaves a residual small enough to correct by exact evolution. After orders $1, \ldots, N_k$ have canceled, the residual in (3.8) contains orders $N_k + 1, \ldots, 2N_k + 2$, including $C_{N_k,t}$ and $d\pi_{N_k}$. Their shifts are at most $110(p+1)$ at order p. The elementary inequality

$$(n+d)! \leq 2^{n+d} n! d! \tag{3.39}$$

separates derivative order from expansion order. It bounds every such coefficient by

$$(P^c)^n (n!)^2 \left[P^c (CN_k)^{300}\right]^{p+1}.$$

Indeed, a shift index $d \leq 110(p+1)$ and $p \leq 2N_k + 2$ give

$$(d!)^2 \leq (CN_k)^{220(p+1)}.$$

There are at most CN_k products at each order. Their sum is covered by

$$(CN_k)\,(CN_k)^{220(p+1)} \leq (CN_k)^{300(p+1)};$$

fixed powers of P and fixed constants raised to $p+1$ are absorbed in the factor $(P^c)^{p+1}$.

The coefficients of κ and κ^2 in W^a are A_1 and $A_2 + B_2 + C_1$. In (3.38), their shift indices are $a_1 = 20$, $a_2 = 120$, and $b_2 = 60$, with C_1 having shift a_1. These indices are independent of N_k. For each such fixed index d, (3.39) gives

$$R^{n+d}((n+d)!)^2 \leq P^c (P^c)^n (n!)^2.$$

Their profiles are also bounded by fixed powers of P, so the same bound applies to these first two velocity coefficients. Since $300\vartheta < 0.01$, enlarging Q in (3.12) ensures

$$P^c (CN_k)^{300} \le k^{0.01}. \tag{3.40}$$

Define the lifted approximate velocity and its transport coefficient by

$$z^a = \kappa^{-1} F^{-1} W^a, \qquad b^a = (\kappa z^a, m_0 \cdot z^a). \tag{3.41}$$

Here z^a is the velocity increment in parent label coordinates, rescaled by κ^{-1}. The first three components of b^a transport y, and its last component transports θ on $\mathbb{R}^3 \times \mathbb{T}$. To sum the derivative bounds, choose a sufficiently small radius $\rho = P^{-c}$ and define

$$\|f\|_\rho = \sum_{n\ge 0} \frac{\rho^n |f|_n}{(n!)^2}. \tag{3.42}$$

The growth bounds above are summable when ρR is sufficiently small; thus ρ is the norm radius corresponding to the growth constant R. The coefficient bounds, with a fixed further shrinking of ρ to sum geometric series, give

$$\|z^a\|_\rho + \|z^a_t\|_\rho + \|\nabla_{y,\theta} z^a\|_\rho \le P^c, \qquad \|b^a\|_\rho \le k^{-1} P^c + O(k^{-1.9}). \tag{3.43}$$

Indeed $m_0 \cdot F^{-1} A_p = m \cdot A_p = 0$, and the mean and C_1 terms of z^a begin with κ. The higher orders sum as $\sum_{p\ge 3} k^{1-p+0.01(p+1)}$. The same calculation gives $\|W^a - \kappa A_1\|_\rho \le k^{-2} P^c$. If r^a denotes the residual after multiplication by $\kappa^{-1} F^{-1}$, then

$$\|r^a\|_\rho \le \exp(-0.7 k^\vartheta \log k) =: \mathcal{R}_k. \tag{3.44}$$

All radius shrinkings and all powers of P used so far are fixed.

3.6. **Correcting the approximate solution.** The normalized residual r^a of the approximation (3.33) satisfies (3.44). Differentiating along the physical graph introduces a factor of k, which complicates estimates for the correction. On $\mathbb{R}^3_y \times \mathbb{T}_\theta$, the transport coefficient b^a is small by (3.43). We solve there for a correction e to the lifted velocity z^a, with zero initial value, and restrict the resulting solution to the physical graph afterward. Throughout this subsection, $s = 6$, $\kappa = k^{-1}$, and

$$D_i = \kappa \partial_{y_i} + (m_0)_i \partial_\theta, \qquad G = F^{-1} F^{-T}, \qquad K = G^{-1} = F^T F. \tag{3.45}$$

The divergence associated with D is $\operatorname{div}_D v := \sum_{i=1}^3 D_i v_i = \kappa \operatorname{div}_y v + m_0 \cdot \partial_\theta v$. Thus a field is divergence-free with respect to D precisely when $\operatorname{div}_D v = 0$. The notation $D \times v$ similarly denotes the curl obtained by replacing each coordinate derivative with D_i. For a vector field v and an integer $r \ge 0$, write

$$|v|_{n,r} = \sum_{I \in \{1,2,3,4\}^n} \|\partial^I v\|_{H^r}.$$

A word I specifies an ordered list of derivatives in (y, θ); for $n = 0$ this is just the H^r norm. Coefficient norms use $W^{r,\infty}$ in place of H^r. All constants in the Gevrey energy estimates below are independent of the cutoff in derivative order and of the auxiliary viscosity.

The preceding estimates give a radius P^{-c} at which $z^a = \kappa^{-1} F^{-1} W^a$, $\partial_t z^a$, and one derivative of z^a have weighted norm at most P^c. At that radius,

$$b^a = (\kappa z^a, m_0 \cdot z^a), \qquad \sum_{n\ge 0} \frac{\rho^n}{(n!)^2} |b^a|_{n,s} \le B_0 \le k^{-1/2}.$$

We decrease the radius by a fixed factor when necessary. The normalized residual r^a has weighted H^s norm at most

$$\mathcal{R}_k = \exp(-0.7k^{\vartheta} \log k).$$

The coefficient bounds, including the fixed number of extra derivatives used below, have the form $P^c R_0^n (n!)^2$, where $R_0 = P^c$.

Take the smooth packet data and hypotheses in §3.2, and impose the smallness condition (3.12), with $Q = Q(c_0)$ fixed sufficiently large and $k \geq k_0(c_0)$ sufficiently large. Let (W^a, q^a) be the truncated expansion (3.33) constructed in the preceding subsection, and let z^a and r^a be its lifted velocity and normalized residual, satisfying (3.43) and (3.44). Set $\Delta_k = \exp(-k^{\vartheta/2})$.

Lemma 3.3. *For the truncated velocity and pressure (W^a, q^a) in (3.33), there exist smooth correction fields e, p_e on $[0, S] \times \mathbb{R}^3_y \times \mathbb{T}_\theta$ satisfying*

$$e(0) = 0, \qquad \operatorname{div}_D e = 0, \qquad D \times p_e = 0,$$

and, at a fixed radius $\rho_* = P^{-c}$,

$$\sup_{0 \leq t \leq S} \left(\|e(t)\|_{\rho_*} + \|e_t(t)\|_{\rho_*} + \|p_e(t)\|_{\rho_*} \right) \leq P^c \Delta_k.$$

There is a smooth scalar $q_e(t, y)$ with

$$\nabla_y q_e(t, y) = \kappa p_e(t, y, km_0 \cdot y).$$

The velocity and pressure defined by

$$\begin{aligned} u^{\text{new}}(t, X(t, \ell y)) &= u(t, X(t, \ell y)) \\ &\quad + \ell \, [W^a + \kappa F e](t, y, km_0 \cdot y). \end{aligned} \tag{3.46}$$

and

$$\begin{aligned} p^{\text{new}}(t, X(t, \ell y)) &= p(t, X(t, \ell y)) \\ &\quad + \ell^2 \left[q^a(t, y, km_0 \cdot y) + q_e(t, y) \right]. \end{aligned} \tag{3.47}$$

form an exact Euler solution on $[0, S]$. The velocity u^{new} is smooth and odd, and its initial increment is

$$u^{\text{new}}(0, \ell y) - u(0, \ell y) = \ell W^a(0, y, km_0 \cdot y).$$

Proof. We first construct the pressure inverse and estimate the correction on $\mathbb{R}^3 \times \mathbb{T}$. We then remove the auxiliary viscosity and restrict to the physical graph to obtain the asserted Euler solution.

The pressure equation. Let $\mathcal{G}$ be the L^2 closure of the fields $D\phi$, with ϕ smooth, periodic in θ, and compactly supported in y. Its orthogonal complement consists exactly of fields satisfying $\operatorname{div}_D v = \sum_i D_i v_i = 0$ in distributions. The orthogonal projection $P_{\mathcal{G}}$ has Fourier symbol

$$\frac{(\kappa\xi + jm_0) \otimes (\kappa\xi + jm_0)}{|\kappa\xi + jm_0|^2}, \qquad (\xi, j) \in \mathbb{R}^3 \times \mathbb{Z},$$

with an arbitrary value on its measure-zero singular set. Thus it commutes with derivatives and has norm at most one on every H^r. Since G is symmetric and $G \geq P^{-c} I$, the operator $P_{\mathcal{G}} G|_{\mathcal{G}}$ is invertible on $\mathcal{G}$ by coercivity. We denote its pressure solution operator by

$$\mathcal{T} f = (P_{\mathcal{G}} G|_{\mathcal{G}})^{-1} P_{\mathcal{G}} f.$$

Here $p = \mathcal{T} f \in \mathcal{G}$ denotes the vector output of the pressure inverse; the physical pressure is scalar. Translation preserves $\mathcal{G}$. Applying spatial difference quotients to $P_{\mathcal{G}}(Gp) = P_{\mathcal{G}} f$

therefore proves the inverse bounds through the fixed Sobolev order s. Differentiating a word of n additional derivatives then gives, for $r = s-1, s$,

$$|p|_{n,r} \le P^c \left(|f|_{n,r} + \sum_{l=1}^{n} \binom{n}{l} R_0^l (l!)^2 |p|_{n-l,r} \right). \tag{3.48}$$

Indeed, every commutator places at least one additional derivative on G; the remaining derivatives fall on p. The same argument at any fixed larger index gives a finite inverse bound, without a claim that its constant is uniform in that index.

Substitution of $W = \kappa F z$ into the lifted Euler equation gives

$$z_t + 2F^{-1}F_t z + z \cdot Dz + \kappa F^{-1}(z \cdot \nabla_y F)z + Gp = 0, \qquad \operatorname{div}_D z = 0. \tag{3.49}$$

Here $p = \kappa^{-2} Dq$ is a vector pressure variable. In particular, $W_t + MW = \kappa F z_t + 2\kappa F_t z$, and $W \cdot \widetilde{d}W = \kappa F(z \cdot Dz) + \kappa^2 (z \cdot \nabla_y F)z$, which verify the factors in this equation. The approximate pressure variable belongs to $\mathcal{G}$: its high part is a differentiated Sobolev potential, and its mean part is an L^2 gradient. The Fourier characterization above covers both cases.

We seek $z = z^a + e$ with $e(0) = 0$. For $0 < \nu \le 1$, first solve

$$e_t + b \cdot \nabla_{y,\theta} e + Z(e) + Gp_e = -r^a + \nu \Delta_{y,\theta} e, \qquad \operatorname{div}_D e = 0, \tag{3.50}$$

where

$$\begin{aligned} b &= (\kappa(z^a + e), m_0 \cdot (z^a + e)), \\ Z(e) &= e \cdot Dz^a + 2F^{-1}F_t e \\ &\quad + \kappa F^{-1}\left[(z^a + e) \cdot \nabla_y F\right](z^a + e) - \kappa F^{-1}(z^a \cdot \nabla_y F) z^a. \end{aligned}$$

Thus Z contains no derivative of e, and $\operatorname{div} b = 0$. We split $p_e = p_0 + p_1$, where

$$p_0 = -\mathcal{T}(Z(e) + r^a), \qquad p_1 = -\mathcal{T}(b \cdot \nabla_{y,\theta} e).$$

The viscosity contributes no pressure because $\operatorname{div}_D(\Delta e) = \Delta(\operatorname{div}_D e) = 0$; the operators D_i have constant coefficients and commute with Δ.

An estimate with a finite derivative cutoff. We will bound the correction uniformly in both the derivative cutoff and the auxiliary viscosity. A slowly decreasing norm radius will absorb the transport and pressure commutators while remaining positive on $[0, S]$. For each word I of additional derivatives, define

$$E_I^2 = \sum_{|\lambda| \le s} \int \langle K \partial^\lambda \partial^I e, \partial^\lambda \partial^I e \rangle, \qquad E_n = \sum_{|I| = n} E_I.$$

These energies are equivalent to $|e|_{n,s}$ with polynomial constants. For $m \ge 0$, a decreasing radius $\rho(t) > 0$, and $w_n = \rho^n / (n!)^2$, set

$$X_m = \sum_{n=0}^{m} w_n E_n, \qquad Y_m = \sum_{n=0}^{m} n w_n E_n.$$

Choose $\rho \le (P^c R_0)^{-1}$. Multiplication estimates and (3.48), with the positive-order coefficient terms absorbed at this radius, give

$$\sum_{n=0}^{m} w_n |p_0|_{n,s} \le P^c (X_m + X_m^2 + \mathcal{R}_k), \tag{3.51}$$

$$\sum_{n=0}^{m} w_n |p_1|_{n,s-1} \le P^c (B_0 + X_m) X_m. \tag{3.52}$$

In the second line the one derivative on e is contained in its base H^s norm. At base index s we instead use the shifted estimate

$$\sum_{j=0}^{m-1}(j+1)w_{j+1}|p_1|_{j,s} \le P^c(B_0+X_m)Y_m. \tag{3.53}$$

To check its derivative count explicitly, the term with l derivatives on b and $j-l$ on ∇e has weight ratio

$$\frac{(j+1)w_{j+1}\binom{j}{l}}{w_l(j-l+1)w_{j-l+1}} = \binom{j+1}{l}^{-1} \le 1.$$

The inverse commutators obey the same ratio. Their coefficient sum is bounded by $P^c\sum_{l\ge1}(\rho R_0)^l$, which is absorbable. Consequently this estimate needs no velocity or pressure derivative beyond the cutoff m.

We next differentiate (3.50) and pair with $K\partial^\lambda\partial^I e$. The highest pressure term vanishes:

$$\langle K\partial^\lambda\partial^I e, G\partial^\lambda\partial^I p_e\rangle = \langle \partial^\lambda\partial^I e, \partial^\lambda\partial^I p_e\rangle = 0.$$

Here $KG = I$, the differentiated velocity satisfies $\operatorname{div}_D(\partial^\lambda\partial^I e) = 0$, and the differentiated pressure belongs to $\mathcal{G}$. A commutator with one of the s base derivatives on G uses only $|p_e|_{n,s-1}$. A commutator with $l \ge 1$ additional derivatives on G uses $|p_e|_{j,s}$, $j = n-l$. For its p_1 part, the relevant ratio is

$$\frac{w_{j+l}\binom{j+l}{l}}{w_l(j+1)w_{j+1}} = \rho^{-1}\frac{j+1}{\binom{j+l}{l}} \le \rho^{-1}.$$

The positive-order coefficient sum is $O(P^c\rho R_0)$, so these pressure terms contribute at most $P^cR_0(B_0+X_m)Y_m$, in addition to the unshifted terms already bounded above.

For transport, integration by parts cancels its highest derivative except for $b\cdot\nabla K$. Base commutators are bounded by $C\|\nabla b\|_{H^{s-1}}\|\nabla\partial^I e\|_{H^{s-1}}$; this follows by the product estimate in H^{s-1}. Commutators involving the additional derivatives have the last displayed weight ratio and contribute at most $P^c\rho^{-1}(B_0+X_m)Y_m$. Differentiating K in time costs P^cX_m. Finally, integration by parts in the heat term gives

$$\nu\langle Kv, \Delta v\rangle = -\nu\sum_a\langle K\partial_a v, \partial_a v\rangle - \nu\sum_a\langle(\partial_a K)v, \partial_a v\rangle \le -\tfrac{1}{2}\nu P^{-c}\|\nabla v\|_2^2 + \nu P^c\|v\|_2^2.$$

Combining these estimates, including the terms in $Z(e)$, yields

$$X_m' \le P^c(X_m + X_m^2 + \mathcal{R}_k) + \left[\frac{\rho'}{\rho} + P^c(\rho^{-1}+R_0)(B_0+X_m)\right]Y_m. \tag{3.54}$$

At zeros of an individual energy we first use $(E_I^2+\epsilon^2)^{1/2}$, then send ϵ to zero at fixed m. All constants in this inequality are independent of m and ν.

Choose

$$\rho(0) = (P^cR_0)^{-1}, \qquad \rho' = -CP^c(B_0+\Delta_k).$$

The fixed exponent in this choice is enlarged to cover all preceding constants. The scale condition $P^Q \le k^{\vartheta/100}$, for a sufficiently large fixed Q, ensures $\rho(t) \ge \rho(0)/2$ on $[0,S]$. Under the bootstrap assumption $X_m \le \Delta_k$, the bracket in (3.54) is nonpositive. Since $X_m(0) = 0$, Gronwall's inequality then gives

$$X_m(t) \le P^cS\exp(P^cS)\mathcal{R}_k < \tfrac{1}{2}\Delta_k.$$

The last inequality follows directly by comparing its logarithm with $-0.7k^{\vartheta}\log k$ and using the same scale condition. Continuity closes the bootstrap uniformly in m and ν.

Existence and removal of viscosity. We construct the correction (e, p_e) asserted in Lemma 3.3 by solving (3.50) for $\nu > 0$ and then passing to $\nu \downarrow 0$. The preceding bound $X_m \le \Delta_k$, obtained from (3.54), extends these viscous solutions to S uniformly in the derivative cutoff. Apply $\mathcal{P}(t) = I - G\mathcal{T}$ to the non-heat terms in (3.50). It is a projection onto the fixed space $\{v : \operatorname{div}_D v = 0\}$ and is the identity on that space. For each fixed $q = s + m$, the projected nonlinearity is locally Lipschitz $H^q \to H^{q-1}$. The heat estimate

$$\|e^{\nu t\Delta} f\|_{H^q} \le C\big(1 + (\nu t)^{-1/2}\big)\|f\|_{H^{q-1}}$$

gives a local mild solution by contraction and continuation while its H^q norm remains bounded. Write e^ν for the viscous solution, and set

$$b^\nu = (\kappa(z^a + e^\nu), m_0 \cdot (z^a + e^\nu)), \qquad f^\nu = -\mathcal{P}(t)\big(b^\nu \cdot \nabla e^\nu + Z(e^\nu) + r^a\big).$$

Then

$$\partial_t e^\nu - \nu\Delta e^\nu = f^\nu, \qquad e^\nu(0) = 0.$$

No time derivative of $\mathcal{P}(t)$ enters this equation. Its range is fixed, and $[D_i, \Delta] = 0$, so the heat flow preserves $\operatorname{div}_D e^\nu = 0$.

On a compact existence interval $I = [t_1, t_2]$, heat maximal regularity gives

$$\|e^\nu\|_{L^2(I;H^{q+1})} + \|\partial_t e^\nu\|_{L^2(I;H^{q-1})} \le C_{\nu,q,I}\left(\|e^\nu(t_1)\|_{H^q} + \|f^\nu\|_{L^2(I;H^{q-1})}\right).$$

The constant may depend on ν; only finiteness is used here. For the inhomogeneous term, the Fourier kernel satisfies

$$\int_0^\infty \nu|\xi, j|^2 e^{-\nu|\xi,j|^2 t}\, dt \le 1.$$

Young's inequality in time gives the two-derivative gain in L^2; low frequencies are bounded on I. Since the source has one spatial derivative, it follows that

$$b^\nu \cdot \nabla e^\nu + Z(e^\nu) + r^a, \quad p_e^\nu \in L^2(I; H^q).$$

This regularity justifies the energy pairings by smoothing, or by the H^{-1}–H^1 pairing at top order. The uniform energy bound extends e^ν to S, and uniqueness at $q = s$ identifies the solutions constructed with different derivative cutoffs.

For every fixed integer $j \ge 0$, the energy bounds and pressure inverse give

$$\sup_{0<\nu\le 1}\left(\|e^\nu\|_{L_t^\infty H^{j+2}} + \|\partial_t e^\nu\|_{L_t^\infty H^j} + \|p_e^\nu\|_{L_t^\infty H^j}\right) \le C_j.$$

Here the two extra derivatives bound the heat term. Local Sobolev compactness and time equicontinuity give a sequence $\nu_l \downarrow 0$ such that, for every finite j,

$$\begin{aligned} e^{\nu_l} &\longrightarrow e \quad \text{in } C([0,S]; H^j_{\mathrm{loc}}), \\ p_e^{\nu_l} &\rightharpoonup^* p_e \quad \text{in } L^\infty([0,S]; H^j), \\ \nu_l \Delta e^{\nu_l} &\longrightarrow 0 \quad \text{in } L^\infty([0,S]; H^j). \end{aligned}$$

The pressure limit remains in the closed gradient space $\mathcal{G}$. Passing to the limit in (3.50) gives

$$e_t + b \cdot \nabla e + Z(e) + Gp_e = -r^a, \qquad \operatorname{div}_D e = 0, \qquad e(0) = 0,$$

where $b = (\kappa(z^a + e), m_0 \cdot (z^a + e))$. For every finite derivative cutoff m, lower semicontinuity gives

$$X_m(e(t)) \le \liminf_{l\to\infty} X_m(e^{\nu_l}(t)) \le \Delta_k.$$

Monotone convergence as $m \to \infty$ proves the full weighted bound. The limit equation and pressure formula give

$$e \in W_t^{1,\infty} H^j \quad (j \ge 0), \qquad p_e = -\mathcal{T}\big(Z(e) + r^a + b \cdot \nabla e\big).$$

Thus the pressure is continuous in each H^j; differentiating these identities gives smoothness in time.

Let $\rho_{\min} = \rho(0)/2 \le \inf_{[0,S]} \rho(t)$ and $\rho_* = \rho_{\min}/2$. The cost of one additional derivative at this smaller radius is bounded by

$$\sup_{n\ge 0} \frac{\rho_*^n((n+1)!)^2}{\rho_{\min}^{n+1}(n!)^2} = \rho_{\min}^{-1} \sup_{n\ge 0}(n+1)^2 2^{-n} \le C\rho_{\min}^{-1} = P^c.$$

The pressure inverse and the limit equation therefore yield

$$\sup_{0\le t\le S} \big(\|e(t)\|_{\rho_*} + \|p_e(t)\|_{\rho_*} + \|e_t(t)\|_{\rho_*}\big) \le P^c \Delta_k.$$

The construction preserves the joint odd parity of the velocity.

Restriction to the physical graph. Put $v^{\mathrm{diag}}(y) = v(y, km_0 \cdot y)$. The chain rule gives $\nabla_y v^{\mathrm{diag}} = \kappa^{-1}(Dv)^{\mathrm{diag}}$ componentwise. In particular, $D \times p_e = 0$ implies $\nabla_y \times p_e^{\mathrm{diag}} = 0$. Since $\mathbb{R}^3$ is simply connected, there is a smooth potential q_e satisfying

$$\nabla_y q_e = \kappa p_e^{\mathrm{diag}}, \qquad dq_e = \kappa F^{-T} p_e^{\mathrm{diag}}.$$

This is exactly the pressure correction required by (3.49). The field $W = W^a + \kappa F e$, restricted to the graph, consequently solves (3.8), including the divergence constraint $\widetilde{d} \cdot W = 0$. Hence the velocity and pressure in (3.46) and (3.47) solve Euler's equation in physical coordinates. For every scalar or vector component v,

$$\int_{\mathbb{R}^3} |v(y, km_0 \cdot y)|^2 \, dy \le C \int_{\mathbb{R}^3} \|v(y,\cdot)\|^2_{H^1(\mathbb{T})} \, dy.$$

Applying this estimate after the chain rule proves every finite spatial Sobolev bound on the graph. The volume-preserving change of coordinates and the bounded smooth matrices F, F^{-1} transfer these bounds to physical space. Higher spatial bounds and the equation give time continuity and smoothness at every finite order. The correction vanishes initially, so the prescribed initial perturbation is retained. This proves Lemma 3.3 and supplies the exact solution asserted in Proposition 3.1. The remaining subsections prove its derivative, particle-map, and initial-data conclusions. □

3.7. **The leading gradient and pressure Hessian.**

Proof of Claim 1 of Proposition 3.1. To prove (3.13) and (3.14), we must control the errors after one derivative of velocity and two derivatives of pressure. Each derivative on the physical graph can cost a factor of k. For the exact normalized velocity $W = W^a + \kappa F e$, differentiating the leading term gives

$$\widetilde{d}_j(\kappa A_{1,i}) = \alpha\chi_1 v_i m_j f'_\delta + \kappa d_j(\alpha\chi_1 v_i) f_\delta.$$

The second term is at most $k^{-1}P^c$. Every other term of W^a has size $k^{-2}P^c$ at a radius P^{-c}. A derivative on the graph costs at most kP^c, so their total differentiated contribution is also

$k^{-1}P^c$. The correction κFe contributes at most $P^c\Delta_k$, where $\Delta_k = \exp(-k^{\vartheta/2})$ is the bound obtained in Lemma 3.3. These bounds prove (3.13) by (3.12).

For the pressure, (3.28) gives

$$\pi_1 = -2\alpha\chi_1 \frac{m \cdot Mv}{D_m} \partial_\theta^{-1} f_\delta.$$

The term in $\widetilde{d}_i\widetilde{d}_j(\kappa^2\pi_1)$ with both derivatives on the angle is therefore

$$\kappa^2 k^2 m_i m_j \partial_\theta^2 \pi_1 = -2\alpha\chi_1(m \cdot Mv)\frac{m_i m_j}{D_m} f_\delta'.$$

Each remaining term has at most one phase derivative $km_i\partial_\theta$, hence is bounded by $k^{-1}P^c$. The higher oscillatory pressures begin with $\kappa^3\pi_2$ and their second graph derivatives sum to the same bound. The mean pressures begin with $\kappa^2\bar{q}_2$; using the estimated gradient $d\bar{q}_p$ and one further derivative d_i bounds their Hessians directly, without estimating the potentials. The error pressure gradient is $\kappa F^{-T}p_e$ on the graph; one more physical derivative costs at most kP^c, giving $P^c\Delta_k$. This proves (3.14). Restoring the physical factors ℓ for velocity and ℓ^2 for pressure cancels the factors from one and two physical derivatives, respectively. $\square$

3.8. **Factorial bounds for the new particle map.**

Proof of Claim 2 of Proposition 3.1. We next prove the particle-map estimate (3.16). Here we assume the parent particle-map bound (3.15). Estimating the new velocity's physical Lipschitz norm and then exponentiating would lose the required frequency bound. We instead use the small transport field b on $\mathbb{R}^3 \times \mathbb{T}$ defined below. For $z = z^a + e$, put

$$b = (\kappa z, m_0 \cdot z).$$

Its derivative word sums in L^∞ and L^2 have bounds $BR_b^n(n!)^2$, where $B \le 2k^{-1/2}$ and $R_b = P^c$. The corresponding bounds for b_t have size and growth constant bounded by fixed powers of P. By increasing Q, we ensure $BR_b \ll 1$. Let $\Phi(t, y, \theta)$ be the flow of b on $\mathbb{R}^3 \times \mathbb{T}$, so $\partial_t\Phi = b(t, \Phi)$ and $\Phi(0, y, \theta) = (y, \theta)$. This flow preserves four-dimensional volume because $\operatorname{div}_{y,\theta} b = 0$.

We give the composition estimate used for Φ. In the ordered derivative formula for a composition, group a word of length n into q nonempty blocks with sizes $j_1, \dots, j_q$ summing to n. When we sum over the ordered sizes, the combinatorial coefficient is $n!/(q!\prod_i j_i!)$. On inserting the factorial bounds for the outer qth derivative and the inner j_ith derivatives, and dividing by $(n!)^2$, the remaining factor is

$$\frac{q!\prod_{i=1}^q j_i!}{n!} \le 1. \tag{3.55}$$

It is one when every $j_i = 1$. Increasing one j_i multiplies the ratio by $(j_i+1)/(n+1) \le 1$, proving the inequality for all block sizes. Sums over component directions are controlled by the word sums themselves.

For a finite truncation of the positive derivative series put

$$U(\zeta) = d\zeta + \sum_{n\ge 1} \frac{\|\partial^n(\Phi - \mathrm{id})\|_\infty}{(n!)^2}\zeta^n,$$

where d is a fixed dimensional constant and ∂^n denotes the sum over words. The integral equation for Φ and (3.55) give coefficientwise

$$U(\zeta) \leq d\zeta + \int_0^t B \frac{R_b U(\zeta)}{1 - R_b U(\zeta)}\, dt' \qquad \text{when } R_b U(\zeta) < 1. \tag{3.56}$$

At $\zeta = (4dR_b)^{-1}$, the initial right side is $1/(4R_b)$. If $R_b U \leq 1/2$, the integral increases $R_b U$ by at most $BR_b S$. The smallness $BR_b \ll 1$ closes the bootstrap, giving $R_b U \leq 1/2$. Returning to the integral equation bounds each coefficient of $\Phi - \mathrm{id}$ by $CBS\zeta^{-n}(n!)^2$; the order-zero bound follows by direct integration of b. The estimates are uniform in the finite truncation, so passing to all orders is justified.

For the L^2 estimate, use the outer factor $(\partial^q b) \circ \Phi$ in L^2 and the inner derivatives in L^∞. Volume preservation leaves its L^2 norm unchanged, and the same series proof applies; order zero again follows by integration. Finally

$$\Phi_t = b \circ \Phi, \qquad \Phi_{tt} = (b_t + (b \cdot \nabla_{y,\theta})b) \circ \Phi.$$

The preceding composition and product estimates at a smaller radius P^{-c} give size and growth constant bounded by fixed powers of P for these two fields in both L^2 and L^∞.

The trajectory $\Phi(t, y, km_0 \cdot y)$ stays on the physical phase graph, because

$$\frac{d}{dt}(\theta - km_0 \cdot y) = m_0 \cdot z - k\kappa m_0 \cdot z = 0.$$

Let $\pi_y : \mathbb{R}^3 \times \mathbb{T} \to \mathbb{R}^3$ be projection onto the first three coordinates, and define the rescaled map

$$Y(t, a) = \ell\, \pi_y \Phi\left(t, \frac{a}{\ell}, \frac{km_0 \cdot a}{\ell}\right). \tag{3.57}$$

Here the last argument is interpreted in $\mathbb{T}$, and $Y(0, a) = a$. The velocity $\kappa z(t, y, km_0 \cdot y)$ of this label flow has zero divergence in y:

$$\mathrm{div}_y \left(\kappa z(t, y, km_0 \cdot y)\right) = \kappa\, \mathrm{div}_y\, z + m_0 \cdot \partial_\theta z = \mathrm{div}_D\, z = 0.$$

Thus Y preserves three-dimensional volume. Each derivative of a graph restriction costs at most Ck; its L^2 bound uses the one-dimensional trace inequality in θ and at most one further derivative on the product space, without an additional graph factor. Rescaling then gives $Y - \mathrm{id}, Y_t, Y_{tt}$ polynomial size and growth constant $k\ell^{-1}P^c$ in both L^2 and L^∞.

The new physical particle map is

$$X^{\mathrm{new}}(t, a) = X(t, Y(t, a)). \tag{3.58}$$

Indeed, differentiating the right side gives the parent velocity plus $F\,Y_t = \ell\kappa F z = \ell W$, as required. We spell out the derivative bound in this last composition. If an inner displacement has size A_i and growth constant R_i, its derivative series is bounded by $(d + 2A_i R_i)\zeta$ when $\zeta \leq (2R_i)^{-1}$. If the outer function has size A_o and growth constant R_o, also impose $R_o(d + 2A_i R_i)\zeta \leq 1/2$. The block estimate (3.55) then bounds the composition by size CA_o at this radius. The outer factor can be placed in L^2 because the inner map preserves volume. Apply this to $X = \mathrm{id} + (X - \mathrm{id})$ and to

$$\begin{aligned} X_t^{\mathrm{new}} &= X_t \circ Y + (\nabla X \circ Y) Y_t, \\ X_{tt}^{\mathrm{new}} &= X_{tt} \circ Y + 2(\nabla X_t \circ Y) Y_t + (\nabla^2 X \circ Y)[Y_t, Y_t] + (\nabla X \circ Y) Y_{tt}. \end{aligned}$$

In factors containing ∇X, split off the identity. All other outer functions have the assumed parent bounds, after finitely many shifts. The resulting size is P^c and growth constant is kP^c.

Passing from L^2 to H^s costs s shifts, hence at most $C_s^{n+1}P^c(kP^c)^{n+s}(n!)^2$. Condition (3.12), after one further fixed enlargement of Q, bounds this by $(k^{C_*})^{n+1}(n!)^2$ with $C_* = 10(s+2)$. This proves (3.16) without a frequency-dependent exponential. □

3.9. **Initial support and the completion of the packet estimate.**

Proof of Claim 3 of Proposition 3.1. It remains to prove the initial-data bounds (3.17) and the support assertions in Proposition 3.1. The correction e in Lemma 3.3 has $e(0) = 0$. Set $y_a = a/\ell$ and $\theta_a = km_0 \cdot a/\ell$, with θ_a interpreted in $\mathbb{T}$, and define

$$\begin{aligned} u_{\mathrm{high},0}(a) &= \ell \sum_{p=1}^{N_k} \big(\kappa^p A_p + \kappa^{p+1} C_p\big)(0, y_a, \theta_a), \\ u_{\mathrm{mean},0}(a) &= \ell \sum_{p=2}^{N_k} \kappa^p B_p(0, y_a). \end{aligned} \tag{3.59}$$

Since $X(0,a) = a$ and $B_1 = 0$, formula (3.46) gives $u^{\mathrm{new}}(0,a) - u(0,a) = u_{\mathrm{high},0}(a) + u_{\mathrm{mean},0}(a)$.

At time zero every oscillatory coefficient retains the factor α, including coefficients solved using a positive history interval. For fixed m, apply (3.39) only at $n \leq m+s+1$. The dependence on the expansion order remains $[P^c(CN_k)^{300}]^{p+1}$; no extra factor $N_k^{c_m}$ is introduced outside this factor depending on the expansion order. Graph derivatives cost at most k^m, and the one-dimensional trace costs one derivative on the product space. This gives the first bound in (3.17), with the harmless physical scaling bounded above by ℓ^{-m}.

The mean initial velocity begins at $\kappa^2 B_2(0)$ and has no angle derivatives. Orders $p \geq 3$ sum as $\sum_{p\geq 3} k^{-p+0.01(p+1)}$; the separate fixed-order bound on B_2 is $k^{-2}P^{c_m}$. This proves the second initial bound. The oscillatory supports are $|a| \leq \ell/2$, and (3.24) gives the mean supports $|a| \leq 2$. The exact correction has zero initial value. If $t_0 = 0$ and $L = 0$, the prescribed forward initial conditions give $A_p(0) = 0$ for every forced $p \geq 2$, hence also $C_p(0) = 0$; the boundary condition gives $B_p(0) = 0$. The initial increment is therefore $\ell(\kappa A_1 + \kappa^2 C_1)(0, y_a, \theta_a)$: the primary oscillation and its curl correction.

Only finitely many polynomial exponents have entered the proof: the fixed-s inverses, the common growth constant, the separation of derivative and expansion orders, the weighted error estimate, and the graph and flow estimates. The only factorial growth with the expansion length was absorbed by $(CN_k)^{300(p+1)}$, with $300\vartheta < 0.01$. Thus a single finite $Q(c_0)$ ensures every use of (3.12). The constants c_m in the initial bounds may depend on the fixed Sobolev order m; their summation over expansion orders uses the same Q. This completes the proof of Proposition 3.1. □

4. Amplification and transfer of the wave geometry

Claim 1 of Proposition 3.1 gives a leading gradient proportional to $v \otimes m$ in (3.13) and a pressure-Hessian increment with coefficient $m \cdot Mv$ in (3.14). Here M is the parent velocity gradient from (3.5), $m = F^{-T}m_0$ is the transported phase normal, and v solves (3.9). We must control both the size and the directions of m, v so that the new gradient can serve as the parent shear for the next packet.

Proposition 4.1 supplies the pressure sign, the new frame $p_2 = m/|m|$, $q_2 = v/|v|$, and bounds comparing the packet's earlier size with its target size. It also bounds the linear map taking arbitrary transverse data from time s to time t, as required by §3.2 (iii). The proof follows m, v in the moving frame of the parent shear (4.3).

4.1. **The parent field and the statement to be proved.** We first specify the parent shear and state the estimates needed for the next packet. We retain the particle map and the matrices F, M, H from (3.5), with the label and component conventions in §2.4. A *ray* is a nonzero vector m satisfying $\dot{m} = -M^T m$; it is the normal to a transported phase surface. A transverse velocity is a vector v with $m \cdot v = 0$ satisfying

$$\dot{v} = -Mv + 2m\frac{m \cdot Mv}{|m|^2}. \tag{4.1}$$

The last term enforces transversality: direct differentiation gives $\frac{d}{dt}(m \cdot v) = 0$.

Let the parent be a smooth odd Euler flow on $[0, S]$, $0 < S \leq 1$, with the particle map and matrices F, M, H in (3.5), localization length $0 < \ell \leq 1$, and activation time $t_0 \in [0, S)$. Impose the following hypotheses.

(i) **Parent shear and frame.** Let $B(t)$ be the gradient at the origin of an older Euler solution. Take orthonormal vectors $p(t), q(t)$ obtained by normalizing, respectively, a ray and a transverse velocity for B, and put $n = p \times q$. The normalization equations are

$$\dot{p} = -B^T p + B_{pp} p, \qquad \dot{q} = -Bq + 2B_{pq} p + B_{qq} q. \tag{4.2}$$

Suppose that on an activation interval $[t_0, S]$ the current parent satisfies

$$M(t, 0) = B(t) + h(t)q(t)p(t)^T + E(t), \qquad \|E(t)\| \leq E_*, \qquad h(t_0) = h_*, \quad \frac{\dot{h}}{h} = -B_{pp} - B_{qq}. \tag{4.3}$$

The rank-one matrix hqp^T sends the old normal p into the old transverse direction q. We assume $\|B\| \leq CG_*$ and $\|\dot{B}\| \leq CG_*^2$, where $G_* \geq 1$.

(ii) **Particle-map bounds.** Let $K_h \geq 2$ bound the parent's physical particle map and its time derivatives as in (3.15). Sobolev embedding, finitely many additional derivatives, and $F^{-1} = \operatorname{cof}(F)^T$ give bounds K_h^c for $F, F^{-1}, F_t, F_{tt}, M, H$ and their first physical-label derivatives. Their higher multiplier bounds have growth constant K_h^c, with the exponent convention in §2.4.

(iii) **Scales and error bounds.** The frozen coefficients $B_{pq}(t_0)$ and $B_{nq}(t_0)$ determine the time scale of the rotation. The parameter x_{prev} records the previous scale; its relation to these coefficients is included below. Choose

$$\begin{gathered} a = B_{pq}(t_0) \in [1/2, 2], \qquad \beta = \frac{B_{nq}(t_0)}{a}, \qquad \frac{1}{2} \leq \beta x_{\text{prev}}^2 \leq 2, \\ \varepsilon = \sqrt{a/h_*}, \qquad \tau = \frac{a(t - t_0)}{\varepsilon}, \qquad x = \sqrt{\beta}\,\tau. \end{gathered} \tag{4.4}$$

Here $0 < \beta \leq \beta_0$ for a sufficiently small absolute constant β_0, and the target is $x = x_{\text{tar}} \geq 2$. We denote the corresponding physical time by t_{tar}. We assume $0 \leq \tau \leq \Theta$, where $\Theta \geq 2 + \beta^{-1/2} + x_{\text{tar}}/\sqrt{\beta}$, and allow at most Θ^{-60} units of τ after the target. Set

$$e_* = C\left(\varepsilon\Theta G_*^2 + E_* + \frac{\ell K_h^c}{\varepsilon}\right), \qquad e_*\Theta^{60} \leq x_{\text{prev}}^{-10}. \tag{4.5}$$

The fixed constant C in this definition is chosen large enough for the estimates below. Equivalently one may use a sufficiently small fixed constant on the right of the smallness condition.

(iv) **History and activation conditions ($t_0 > 0$).** Assume the packet coercivity condition (3.11) and, on $[0, t_0]$,

$$\|M\|_\infty \le C_M h_*, \qquad \|H\|_\infty \le C_H h_* h_{\text{old}}, \qquad 1 \le h_{\text{old}} \le h_*, \qquad t_0^{-1} \le h_*. \tag{4.6}$$

At activation write $\overline{B} = B(t_0) + E(t_0)$ and require

$$\overline{B}_{pp} < 0, \qquad \|\overline{B}\| \le \zeta h_*. \tag{4.7}$$

The fixed number $\zeta > 0$ is chosen sufficiently small in terms of C_M, C_H. Finally $t_0^{-1} \le K_h^c$ when $t_0 > 0$.

Choose $m_0 = F(t_0, 0)^T n / |F(t_0, 0)^T n|$ and $m = F^{-T} m_0$. Here n is evaluated at t_0.

Proposition 4.1. *For every parent flow satisfying the four hypotheses in §4.1, there is a primary transverse velocity v with the following properties. When $t_0 > 0$, it has the form $v = FR_\perp \xi_t$ on $[0, t_0]$, where $FR_\perp \xi$ is the stationary displacement with $\xi(0) = 0$ and $\xi(t_0) = \xi_T$, as prescribed in §3.2.*

1. **Activation data and pressure sign.** *Its central activation data satisfy*

$$v_q(t_0, 0) = 1, \qquad -C \le v_p(t_0, 0) \le 0. \tag{4.8}$$

For $t_0 = 0$ we take $v(t_0) = q$. On every label $|y| \le 1/2$,

$$m \cdot Mv > 0 \qquad (\tau \ge 1). \tag{4.9}$$

2. **Frame transfer and compression.** *At the central target time define $p_2 = m/|m|$, $q_2 = v/|v|$, $n_2 = p_2 \times q_2$ and $a_2 = p_2 \cdot Mq_2$, $\beta_2 = (n_2 \cdot Mq_2)/a_2$. Then*

$$\begin{aligned} \frac{a_2}{a} &= 1 + O\left(x_{\text{tar}}^{-4} + \frac{\beta}{x_{\text{tar}}^2} + \frac{\sqrt{\beta}}{x_{\text{tar}}^3} + e_* \Theta^{40} \right), \\ \beta_2 x_{\text{tar}}^2 &= 1 + O\left(\sqrt{\beta} + x_{\text{tar}}^{-4} + e_* \Theta^{40} \right), \end{aligned} \tag{4.10}$$

and

$$p_2 \cdot Mp_2 \le -\frac{c\sqrt{h_*}}{x_{\text{prev}} x_{\text{tar}}} + C(G_* + E_*). \tag{4.11}$$

3. **Relative sizes.** *The size estimates below hold for an absolute constant $b > 0$. Write $A_{\text{tar}} = |m(t_{\text{tar}}, 0)||v(t_{\text{tar}}, 0)|$. Uniformly on the packet support, $|m||v|/A_{\text{tar}} \le C$ for $\tau \ge 1$, whereas on the history interval and for $0 \le \tau < 1$,*

$$\frac{|m||v|}{A_{\text{tar}}} \le K_h^c \Theta^c \varepsilon^{-c} \exp(-b x_{\text{prev}}). \tag{4.12}$$

4. **Propagator and normalization.** *There is a positive scalar function g, with $g(t_0) = 1$, for which the propagator for arbitrary transverse initial data, expressed in the packet coordinates $A = FR_\perp a$, has operator norm at most $P^c g(t)/g(s)$, $t_0 \le s \le t \le S$. For any prescribed child shear h_{child}, the normalization*

$$\alpha = \frac{\delta h_{\text{child}}}{A_{\text{tar}}} \tag{4.13}$$

satisfies $\alpha \le P^c e^{-b x_{\text{prev}}}$ and $\sup_{[t_0, S]} \alpha g \le P^c$. Here P contains $K_h, \varepsilon^{-1}, \Theta, h_{\text{child}}, \delta^{-1}$ and, when applicable, t_0^{-1}, or polynomial upper bounds for them.

The bounds on the transverse propagator and on αg verify §3.2 (iii), which is required to apply Proposition 3.1. At the central target point, $\chi_1 = 1$ and $f'_\delta(0) = \delta^{-1}$, so its leading gradient increment is

$$\alpha\delta^{-1} v \otimes m = \frac{h_{\text{child}}}{|m||v|} v \otimes m = h_{\text{child}} q_2 p_2^T. \tag{4.14}$$

Thus (3.13), with its stated error, produces a shear in the new frame. The sign in (4.9) fixes the sign of the coefficient multiplying f'_δ in (3.14). The remaining conclusions describe the new frame and compare the packet's earlier size with its target size. We first choose the activation velocity, then prove growth and stability, and finally calculate the transferred parameters.

4.2. **Choosing the velocity at the activation time.**

Proof of Proposition 4.1. We first prove the activation-data assertion in Claim 1 of Proposition 4.1. The forward analysis then uses only the endpoint condition (4.8). Let $s_0 > 0$ be defined by $m(t_0, 0) = s_0 n$. The bounds for $F^{\pm 1}$ give $s_0 + s_0^{-1} \leq K_h^c$. Suppose $t_0 > 0$. For an endpoint $Y \in n^\perp$ consider the stationary transverse displacement η from $\eta(0) = 0$ to $\eta(t_0) = Y$, with action

$$\mathcal{E}(\eta) = \int_0^{t_0} (|\eta_t|^2 - H\eta \cdot \eta)\, dt.$$

The pointwise variational inverse (3.26) constructs it. Since $\int |\eta|^2 \leq (t_0^2/2) \int |\eta_t|^2$, the coercivity condition gives $\mathcal{E}(\eta) \geq \frac{1}{2} \int |\eta_t|^2$ for paths starting at zero. The stationary path minimizes the action among paths with its endpoints.

Integration by parts in the stationary equation shows that the endpoint quadratic form is $Y \cdot \Lambda Y$, where $\Lambda Y = \operatorname{proj}_{n^\perp} \eta_t(t_0)$. Polarization proves symmetry, and the preceding inequality proves $\Lambda \geq 0$. To bound its norm, let

$$L_0 = t_0^{-1} + \|M\|_\infty + \|H\|_\infty^{1/2} + 1.$$

An admissible comparison path is zero until $t_0 - L_0^{-1}$ and then equals a linear ramp times the orthogonal projection of Y onto $m(t)^\perp$. The derivative of this projection is bounded by $C\|M\|_\infty$. Its absolute action is therefore at most

$$C \left(L_0 + \frac{\|M\|_\infty^2}{L_0} + \frac{\|H\|_\infty}{L_0} \right) |Y|^2 \leq C_0 h_* |Y|^2.$$

Consequently $0 \leq \Lambda \leq C_0 h_* I$.

The velocity $w = \eta_t - M\eta$ is transverse. At the endpoint its two coordinates are $(\Lambda - \operatorname{proj}_{n^\perp} M)Y$. Write $b = \Lambda_{pq}$, $d = \Lambda_{qq}$ and $u = \Lambda_{pp} - \overline{B}_{pp} > 0$. If $b \leq h_*/2$, we take $Y = -p$, obtaining

$$w_p = -u \leq 0, \qquad w_q = h_* + \overline{B}_{qp} - b \geq h_*/3.$$

If $b > h_*/2$, positivity gives $\Lambda_{pp} \geq b^2/\Lambda_{qq} \geq h_*/(4C_0)$. We take $Y = q - (b - \overline{B}_{pq})p/u$. Then $w_p = 0$ and

$$\begin{aligned} w_q &= d - \overline{B}_{qq} - \frac{(b - h_* - \overline{B}_{qp})(b - \overline{B}_{pq})}{u} \\ &= \left(d - \frac{b^2}{u} \right) - \overline{B}_{qq} + \frac{b^2 - (b - h_* - \overline{B}_{qp})(b - \overline{B}_{pq})}{u}. \end{aligned}$$

The first bracket is nonnegative, since $u \geq \Lambda_{pp}$. The numerator in the last term is

$$bh_* + b(\overline{B}_{pq} + \overline{B}_{qp}) - h_*\overline{B}_{pq} - \overline{B}_{qp}\overline{B}_{pq} \geq h_*^2/2 - C(C_0+1)\zeta h_*^2.$$

Together with $u \leq (C_0+\zeta)h_*$, this proves $w_q \geq ch_*$ after fixing ζ. In either case division of the path and its endpoint by w_q produces (4.8) and $|Y| \leq C/h_*$. The prescribed label-coordinate endpoint is $\xi_T = R_\perp^T F(t_0,0)^{-1}Y$; indeed $m_0 \cdot F^{-1}Y = m \cdot Y = 0$.

We use this same ξ_T at neighboring labels. Here it matters that the history solution has polynomial bounds in the *parent* parameters. Subtracting $t\xi_T/t_0$ reduces its equation to one with zero endpoints; the coercive estimate gives $\|\xi_t\|_{L_t^2} \leq K_h^c$. Subtracting the weak equations at labels $\mathsf{a}_1, \mathsf{a}_2$ gives the same estimate for their difference, multiplied by $|\mathsf{a}_1 - \mathsf{a}_2|$, since every coefficient difference is at most $K_h^c|\mathsf{a}_1 - \mathsf{a}_2|$. The strong matrix equation (3.27) then bounds ξ_{tt} and its difference in L_t^2. The one-dimensional time trace inequality and multiplication by $FR_\perp$ show

$$\sup_{[0,t_0]}|v| \leq K_h^c, \qquad \sup_{[0,t_0]}|v(t,\mathsf{a}_1) - v(t,\mathsf{a}_2)| \leq K_h^c|\mathsf{a}_1 - \mathsf{a}_2|.$$

The envelope can now be multiplied in as in the packet construction. The activation data are now fixed. To complete Claim 1 of Proposition 4.1, we must establish the sign condition (4.9) during forward evolution.

4.3. **The rotating frame and the leading equations.** We now evolve the activation data (4.8) using the ray and velocity equations (2.3). In the frame (p,q,n) of (4.2), the large shear hqp^T in (4.3) occupies a single matrix entry. Because this frame moves with the older flow, the change of coordinates also contributes a rotation term to the time derivatives. The scaling $h_*\varepsilon^2 = a$ from (4.4) normalizes the leading shear coefficient in these equations.

Let R_f have columns (p,q,n) and set $S_f = R_f^T\dot{R}_f$. Differentiating (4.2) gives

$$(S_f)_{12} = B_{pq}, \qquad (S_f)_{13} = B_{pn}, \qquad (S_f)_{32} = -B_{nq}, \qquad S_f^T = -S_f.$$

We use this central frame on neighboring trajectories too. Their parent gradients differ from $B + hqp^T$ by at most $E_* + \ell K_h^c$. The component columns and the gradient matrix in this frame are

$$\widehat{m} = R_f^T m, \qquad \widehat{v} = R_f^T v, \qquad \widehat{M} = R_f^T M R_f.$$

Since $\dot{R}_f^T = -S_f R_f^T$, differentiation gives

$$\dot{\widehat{m}} = -(\widehat{M} - S_f)^T\widehat{m}, \qquad \dot{\widehat{v}} = -(\widehat{M} + S_f)\widehat{v} + 2\widehat{m}\frac{\widehat{m}\cdot\widehat{M}\widehat{v}}{|\widehat{m}|^2}. \tag{4.15}$$

We suppress the hats in the component calculations below. Scalar products and norms are unchanged because the frame is orthonormal. Introduce scaled components by

$$m/s_0 = (P, \varepsilon Q, N), \qquad v = (\varepsilon U, V, \varepsilon W). \tag{4.16}$$

In physical vectors these formulas read $m = s_0(Pp + \varepsilon Qq + Nn)$ and $v = \varepsilon Up + Vq + \varepsilon Wn$. The letters P, Q, N, U, V, W in this section denote component functions; in particular this P is distinct from the packet data bound in §3. Transversality is the identity $PU + QV + NW = 0$. At the center $(P,Q,N) = (0,0,1)$ and $(U,V) = (-\lambda, 1)$ initially, where $0 \leq \lambda \leq C/\varepsilon$. The corresponding neighbor errors are at most $\ell K_h^c/\varepsilon$.

A prime now denotes $d/d\tau$. The leading ray system and its solution are

$$P' = -Q, \quad Q' = -2\beta N, \quad N' = 0; \qquad P_0 = \beta\tau^2 = x^2, \quad Q_0 = -2\beta\tau, \quad N_0 = 1. \tag{4.17}$$

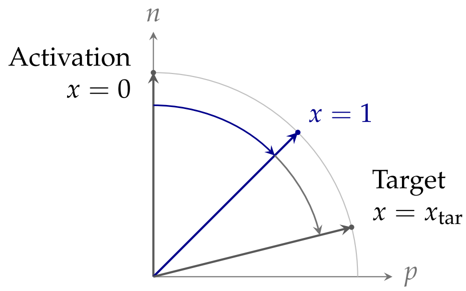

$$\frac{x^2 p + n}{\sqrt{1 + x^4}}$$

Normalized projection onto the moving (p, n) plane.

$0 \le x \le 1$: amplitude amplification (Equation (4.22)).

$x = x_{\mathrm{tar}} \ge 2$: form the next frame (Equation (4.10)).

FIGURE 2. The normalized projection of the ideal ray turns from n toward p. The marked positions show activation, the end of the main growth interval, and a finite transfer target. The target ray is drawn at $x_{\mathrm{tar}} = 2$; the estimates allow any $x_{\mathrm{tar}} \ge 2$. The full vector is $x^2 p - 2\varepsilon\sqrt{\beta}\, xq + n$, and the transverse velocity remains perpendicular to this full vector. The rays have unit length; the velocity amplitude is not shown.

Figure 2 shows its normalized projection onto the (p, n) plane. We record why the errors are small despite the large shear. Its scaled coefficient obeys $\varepsilon^2 h/a = 1 + O(\varepsilon\Theta G_*)$. The entries $(M - S_f)_{12}$ and $(M - S_f)_{32}$ are respectively $O(E_* + \ell K_h^c)$ and $2B_{nq} + O(E_* + \ell K_h^c)$. The moving entries B_{pq}, B_{nq} change by $O(\varepsilon\Theta G_*^2)$, including frame rotation. All remaining scaled coefficients contain either an error or a factor $\varepsilon O(G_*)$. Thus the exact ray system differs entrywise from (4.17) by at most Ce_*. The triangular ideal propagator has norm $C\Theta^2$. Duhamel's formula, $|(P_0, Q_0, 1)| \le C\Theta^2$, and $e_*\Theta^3 \ll 1$ give

$$|P - P_0| + |Q - Q_0| + |N - 1| \le Ce_*\Theta^5, \qquad N \ge 1/2. \tag{4.18}$$

The lower bound for N now allows us to solve the transversality identity:

$$W = -\frac{PU + QV}{N}.$$

It remains to estimate the two independent velocity components U, V. Set $D_a = P^2 + \varepsilon^2 Q^2 + N^2$ and $J = (m/s_0) \cdot Mv/a$. For arbitrary (U, V) we have

$$\begin{aligned}
|W| &\le C\Theta^2(|U| + |V|), \\
|D_a - (1 + P_0^2)| &\le Ce_*\Theta^7, \\
|J - [(P_0 + \beta)V + Q_0 U]| &\le Ce_*\Theta^5(|U| + |V|).
\end{aligned} \tag{4.19}$$

For the last estimate the three leading row contributions are

$$\frac{PB_{pq}V}{a}, \qquad \frac{h\varepsilon^2}{a}QU, \qquad \frac{NB_{nq}V}{a}.$$

Every other term contains an error or $\varepsilon O(G_*)$ and at most $C\Theta^4(|U| + |V|)$. The unprojected term in U' is $-2V + O(e_*\Theta^2)(|U| + |V|)$, and its projected term is $2PJ/D_a$. The main term in V' is $-U$; all remaining terms, including $2\varepsilon^2 QJ/D_a$, are bounded by $Ce_*\Theta^4(|U| + |V|)$. Using $D_a \ge 1/4$ in these rational expressions gives a matrix error at most $Ce_*\Theta^{12}$ from

$$U' = -2V + \frac{2P_0[(P_0 + \beta)V + Q_0 U]}{1 + P_0^2}, \qquad V' = -U. \tag{4.20}$$

In particular, with the scalar $D = 1 + P_0^2$ and $D' = -2P_0Q_0$, we obtain

$$(DV')' = 2(1 - \beta P_0)V. \tag{4.21}$$

4.4. **Growth of the ideal velocity.** For the ideal system (4.20), we first estimate amplification up to $x = 1$ and then control the direction ratio U/V up to the target $x = x_{\mathrm{tar}}$. Let V_λ solve (4.21) with $V_\lambda(0) = 1$ and $V_\lambda'(0) = \lambda \geq 0$. Its companion velocity component is $U_\lambda = -V_\lambda'$. On $0 \leq x \leq 1$, the right side is positive while $V_\lambda > 0$, so integration preserves positivity and monotonicity. Since $x = \sqrt{\beta}\,\tau$, this region lasts for a scaled time $\beta^{-1/2}$. The bounds $D \leq 2$ and $2(1 - \beta P_0) \geq 1$ turn this long interval of growth into quantitative amplification:

$$V_\lambda(\tau) \geq 1 + \frac{\lambda}{2}\tau + \frac{1}{2}\int_0^\tau (\tau - s)V_\lambda(s)\,ds \geq \cosh(\tau/\sqrt{2}).$$

The second inequality follows by iteration of the positive integral kernel. Consequently

$$V_\lambda(x = 1) \geq \exp(b_0/\sqrt{\beta}). \tag{4.22}$$

On this interval $l = V_\lambda'/V_\lambda$ satisfies $l' \leq 2 - l^2$ and $l \geq 0$. Comparison gives $l(\tau) \leq \sqrt{2}\coth(\sqrt{2}\tau)$, uniformly in λ, for $\tau > 0$.

Beyond $x = 1$ we need both a lower bound for the amplitude and an estimate for its direction ratio U/V. A reciprocal variable sends this range to a bounded interval and keeps the right-hand coefficient of the transformed scalar equation positive. First rewrite the equation as

$$\big((1 + x^4)V_x\big)_x = (2/\beta - 2x^2)V.$$

Set $\rho = 1/x$ and $f(\rho) = V(1/\rho)/\rho$. In particular $V(x) = \rho f(\rho)$ and $V_x = -\rho^2 f - \rho^3 f_\rho$. Substitution yields

$$\big((1 + \rho^4)f_\rho\big)_\rho = (2/\beta - 2\rho^2)f.$$

Since $f(1) > 0$ and $f_\rho(1) = -V(1) - V_x(1) < 0$, the identity

$$(1 + \rho^4)f_\rho(\rho) = 2f_\rho(1) - \int_\rho^1 (2/\beta - 2s^2)f(s)\,ds$$

preserves $f_\rho < 0$ as we integrate backwards, and hence preserves $f > 0$. Thus $xV(x) = f(1/x)$ is increasing. Since $U = -V'$, the direction ratio U/V can be recovered from a logarithmic derivative. Define

$$z = -\sqrt{\beta}\,f_\rho/f, \qquad \mu(\rho) = \sqrt{\frac{2 - 2\beta\rho^2}{1 + \rho^4}}, \qquad \sigma = 1 - \rho.$$

Direct logarithmic differentiation gives

$$\sqrt{\beta}\,z_\sigma = \mu^2 - z^2 + \sqrt{\beta}\frac{4\rho^3}{1 + \rho^4}z. \tag{4.23}$$

The first two terms on the right cancel at $z = \mu$. We compare z with this positive root to obtain the direction estimate. At $\rho = 1$, $z = \sqrt{\beta} + l(x = 1)$ is uniformly bounded. Equation (4.23) preserves $z \geq 0$ and gives a uniform upper bound. For $w = z - \mu$ it becomes

$$\sqrt{\beta}\,w_\sigma = -(z + \mu)w + \sqrt{\beta}\left(\frac{4\rho^3}{1 + \rho^4}z - \mu_\sigma\right).$$

The bracket is bounded and $z+\mu \geq c > 0$. Multiplication by the integrating factor therefore gives $|w| \leq Ce^{-c(1-\rho)/\sqrt{\beta}} + C\sqrt{\beta}$. In particular, uniformly in $\lambda \geq 0$,

$$z^2 = \frac{2}{1+\rho^4} + O(\sqrt{\beta}) \quad (0 \leq \rho \leq 1/2), \qquad r_\lambda := \frac{U_\lambda}{V_\lambda} = \begin{cases} -l, & x \leq 1, \\ \sqrt{\beta}/x - z/x^2, & x \geq 1. \end{cases} \tag{4.24}$$

For $\tau \geq 1$ these formulas bound $|r_\lambda|$ by an absolute constant. The ideal solution now has the required growth and direction estimates. These are the inputs to Section 4.5, where we prove the sign assertion in Claim 1 of Proposition 4.1 and obtain the propagator estimate needed for Claim 4 of Proposition 4.1.

4.5. **Stability relative to the growing solution.** We compare the exact scaled components (4.16) with the ideal system (4.20). This proves the pressure sign and the propagator bound in Claims 1 and 4 of Proposition 4.1. In this subsection V_0 is the ideal solution with zero initial slope. In the propagator calculation, s, t denote scaled times. A small coefficient error acts throughout an interval on which the ideal solution grows exponentially. Measuring the propagator in units of $V_0(t)/V_0(s)$ accounts for this growth and leaves an error controlled by powers of Θ. We need this comparison for arbitrary transverse data to supply the assumption in §3.2 (iii). Reduction of order makes the comparison explicit; for V_λ, it gives

$$V_\lambda = V_0(1+\lambda I), \qquad I(\tau) = \int_0^\tau \frac{du}{D(u)V_0(u)^2}, \qquad I(1) \geq c > 0. \tag{4.25}$$

The last bound follows from uniformly bounded ideal coefficients on $0 \leq \tau \leq 1$. Monotonicity before $x = 1$, and monotonicity of xV_0 afterwards, show that $V_0(s)/V_0(u) \leq C\Theta$ for $s \leq u$. Its logarithmic derivative l_0 is uniformly bounded on the whole interval, including $\tau < 1$ since its initial slope is zero.

For arbitrary data $Y(s), Y'(s)$, another form of reduction of order is

$$Y(t) = \frac{V_0(t)}{V_0(s)} \left[Y(s) + D(s)(Y'(s) - l_0(s)Y(s)) \int_s^t \frac{(V_0(s)/V_0(u))^2}{D(u)}\, du \right]. \tag{4.26}$$

The integral is at most $C\Theta^3$ and $D(s) \leq C\Theta^4$. After extracting the same factor $V_0(t)/V_0(s)$, differentiation adds a bounded multiple of the bracket and the term

$$\frac{D(s)}{D(t)}(Y'(s) - l_0(s)Y(s)) \left(\frac{V_0(s)}{V_0(t)} \right)^2,$$

whose size is at most $C\Theta^6(|Y(s)| + |Y'(s)|)$. Thus the ideal two-component propagator Φ_0 satisfies

$$\|\Phi_0(t,s)\| \leq C\Theta^8 V_0(t)/V_0(s).$$

If ΔA is the exact matrix error, then $\|\Delta A\| \leq Ce_*\Theta^{12}$. Duhamel's formula in the norm weighted by $V_0(t)/V_0(s)$ has integral operator norm at most $Ce_*\Theta^{8+12+1} = Ce_*\Theta^{21} \ll 1$. Summing the iterated Duhamel terms gives $\|\Phi(t,s)\| \leq 2C\Theta^8 V_0(t)/V_0(s)$. For the primary data, including their neighbor error, it also gives

$$|U - U_\lambda| + |V - V_\lambda| \leq Ce_*\Theta^{29}(1+\lambda)V_0(t). \tag{4.27}$$

Indeed the initial error contributes $Ce_*\Theta^8 V_0$; the inhomogeneous term is bounded by

$$Ce_*\Theta^{12+8+8+1}(1+\lambda)V_0.$$

For $\tau \geq 1$, (4.25) gives $V_\lambda \geq c(1+\lambda)V_0$. Hence

$$V > 0, \qquad V/V_\lambda = 1 + O(e_*\Theta^{29}), \qquad r := U/V = r_\lambda + O(e_*\Theta^{29}).$$

With $w_3 = W/V = -(Pr + Q)/N$, it follows that $w_3 = -P_0 r_\lambda - Q_0 + O(e_*\Theta^{31})$, and therefore

$$J/V = P_0 + \beta + Q_0 r_\lambda + O(e_*\Theta^{33}). \tag{4.28}$$

The leading expression is at least β for $x \le 1$ because $Q_0 r_\lambda \ge 0$. For $x \ge 1$ it equals $x^2 - \beta + 2\sqrt{\beta}z/x > 0$. Condition (4.5), together with $\beta \asymp x_{\text{prev}}^{-2}$, makes the error smaller than half these lower bounds. Since $m \cdot Mv = s_0 aJ$, this proves (4.9). Together with the activation construction, this completes Claim 1 of Proposition 4.1. The relative error estimates also give the component bounds used in the target comparisons below.

4.6. **The next frame and the size comparisons.** It remains to prove Claims 2–4 of Proposition 4.1: the target frame and compression, the relative sizes, and the propagator and normalization bounds. We use the component ratios $r = U/V$ and $w_3 = W/V$ estimated in §4.5, together with the bound for J/V in (4.28).

Frame transfer and compression. At the target, normalizing m and v removes their amplitudes from a_2 and β_2. This reduces the transfer calculation to the component estimates above. With $E_v = 1 + \varepsilon^2(r^2 + w_3^2)$ and $T = M(v/V)/a$, the definitions of p_2, q_2 give

$$\frac{a_2}{a} = \frac{J/V}{\sqrt{D_a}\sqrt{E_v}}, \qquad \beta_2 = \frac{[(P, \varepsilon Q, N) \times (\varepsilon r, 1, \varepsilon w_3)] \cdot T}{(J/V)\sqrt{E_v}}. \tag{4.29}$$

The preceding estimates imply $T_p = 1 + O(e_*\Theta^2)$, $T_n = \beta + O(e_*\Theta^2)$, and $\varepsilon T_q = r_\lambda + O(e_*\Theta^{31})$. The cross product is $(-N + \varepsilon^2 Q w_3, \varepsilon(Nr - Pw_3), P - \varepsilon^2 Qr)$. Its leading dot product is consequently

$$\begin{aligned} -1 + \beta P_0 + (1 + P_0^2) r_\lambda^2 + P_0 Q_0 r_\lambda &= -1 + (1 + \rho^4) z^2 + \beta\rho^2 - 2\sqrt{\beta} z \rho^3 \\ &= 1 + O(\sqrt{\beta}), \qquad \rho = 1/x \le 1/2. \end{aligned}$$

The first equality follows by inserting $P_0 = x^2$, $Q_0 = -2\sqrt{\beta}x$, and $r_\lambda = \sqrt{\beta}/x - z/x^2$; the βx^2 and $\sqrt{\beta}xz$ terms cancel. The accumulated error in this numerator is at most $Ce_*\Theta^{36}$, using $|P| \le C\Theta^2$, $|Q| \le C\Theta$, $|w_3| \le C\Theta^2$ and $\varepsilon \le Ce_*$. Also

$$J/V = x^2 - \beta + 2\sqrt{\beta}z/x + O(e_*\Theta^{33}), \quad D_a = 1 + x^4 + O(e_*\Theta^7), \quad E_v = 1 + O(\varepsilon^2\Theta^4).$$

Substitution in (4.29) proves (4.10). The compression is calculated directly from the shear:

$$p_2 \cdot Mp_2 = \frac{h\varepsilon QP}{D_a} + O(G_* + E_*).$$

At the target, (4.18) gives $QP \le -c\sqrt{\beta}x_{\text{tar}}^3$ and $D_a \le Cx_{\text{tar}}^4$, while $h \asymp h_*$ and $h_*\varepsilon = \sqrt{ah_*}$. Since $\sqrt{\beta} \asymp x_{\text{prev}}^{-1}$, this proves (4.11).

Relative sizes. We now prove Claim 3 of Proposition 4.1. For $\tau \ge 1$, uniformly on neighboring labels,

$$|m||v| \asymp s_0\sqrt{1 + x^4}\, V_\lambda.$$

This ideal size is bounded by a fixed multiple of its target value: V_λ increases up to $x = 1$, and afterwards $x^2 V_\lambda = xf(1/x)$ increases. The logarithmic derivative of the latter with respect to τ is $\sqrt{\beta}/x + z/x^2$, which is bounded; the allowed extra interval after the target changes size by a fixed factor. On the history interval $|m||v| \le K_h^c$, and for $\tau < 1$ it is at most $K_h^c\Theta^c\varepsilon^{-c}$. In contrast,

$$V_\lambda(x_{\text{tar}}) \ge V_\lambda(1)/x_{\text{tar}} \ge x_{\text{tar}}^{-1} e^{b_0/\sqrt{\beta}}.$$

These inequalities prove (4.12).

Propagator and normalization. To finish Claim 4 of Proposition 4.1, we convert the propagator bound to the packet coordinates and apply the target normalization. Finally choose $g(t) = V_\lambda(a(t-t_0)/\varepsilon)$. Since I is increasing, (4.25) implies $V_0(t)/V_0(s) \le V_\lambda(t)/V_\lambda(s)$. Changing from (U,V) to physical transverse vectors and then to the coordinates $FR_\perp$ costs only $K_h^c\varepsilon^{-1}\Theta^c$. The propagator estimate therefore has the required form $P^c g(t)/g(s)$, even before $\tau = 1$. The target lower bound and (4.13) give $\alpha \le P^c e^{-bx_{\text{prev}}}$. The preceding size comparisons, or the same monotonicity estimates for V_λ alone, give $\sup \alpha g \le P^c$. This completes the proof of Proposition 4.1. □

5. Choosing the scales and iterating the construction

We combine the packet construction of Proposition 3.1 with the amplification and frame transfer in Proposition 4.1 to construct the sequence in (2.6). Repeating the amplification requires each new shear to dominate its predecessor before the parent's existence interval ends. Meanwhile, the changes to the initial datum must remain summable in every fixed Sobolev norm. The exponential separation between initial and target sizes in (4.12) allows the scales to meet these demands while retaining the pressure, initial gradient, and particle-map bounds needed for another step. For each approximating exact solution U^i with pressure p_i, write $M_i = \nabla U^i$ and $H_i = \nabla^2 p_i$. Norms of these fields are taken over physical space and the time interval under discussion.

5.1. **A smooth starting flow and local existence.** We construct a base solution U_B whose central gradient gives $a = 1$ and $\beta = x_0^{-2}$ in the geometric parameters (4.4). Localizing the vector potential of a linear velocity field gives a compactly supported, divergence-free datum with the required gradient near the origin.

Fix an oriented orthonormal basis (p,q,n), with $n = p \times q$. A large number x_0 will be fixed last. Define the trace-free linear map

$$L_B q = p + x_0^{-2} n, \qquad L_B p = L_B n = 0.$$

Choose an even, compactly supported Gevrey cutoff χ_B, equal to one on a fixed neighborhood of the origin, and set

$$u_{B,0}(a) = \operatorname{curl}\left(-\frac{1}{3}\chi_B(a)\, a \times L_B a\right). \tag{5.1}$$

Here "Gevrey" means that its derivatives satisfy bounds $C^{r+1}(r!)^2$. Since $\operatorname{curl}(a \times L_B a) = -3L_B a$, this is a divergence-free, odd field equal to $L_B a$ near zero. Its support and all its factorial Sobolev bounds are uniform for $x_0 \ge 1$.

We record the local theory used both here and at the end of the proof. For smooth divergence-free data, the projected Euler equation has a unique smooth solution on an interval whose length is bounded below in terms of the initial H^3 norm. Its energy estimates are

$$\frac{d}{dt}\|u(t)\|_{H^m} \le C_m \|\nabla u(t)\|_{L^\infty} \|u(t)\|_{H^m}, \qquad m \ge 3, \quad m \in \mathbb{N}. \tag{5.2}$$

For completeness, apply a Fourier projection to $|\xi| \le N$ to the projected equation. This gives a locally Lipschitz ordinary differential equation on the band-limited subspace of H^m, with initial datum $u_N(0) = \Pi_N u_0$. Orthogonality of the projection preserves the transport cancellation. For a commutator product with derivative orders j and $m-j+1$, interpolate between $\nabla u \in L^\infty$ and $\nabla^m u \in L^2$, using

$$\|\nabla^j u\|_{L^{2(m-1)/(j-1)}} \le C_m \|\nabla u\|_{L^\infty}^{1-(j-1)/(m-1)} \|\nabla^m u\|_{L^2}^{(j-1)/(m-1)}.$$

The endpoint $j = 1$ has exponent ∞. The two interpolation powers add to one. The same calculation at each lower differentiated order, together with conservation of the undifferentiated energy, proves (5.2). The embedding $H^3(\mathbb{R}^3) \hookrightarrow C_b^1(\mathbb{R}^3)$ gives a common interval for all truncations; (5.2) then bounds every higher norm there. Their residual in the untruncated equation satisfies

$$\|r_N\|_{L^2} \le CN^{-(m-1)}\|u_N \cdot \nabla u_N\|_{H^{m-1}}.$$

The L^2 difference energy therefore gives convergence in $C_t L_x^2$. Interpolation with the uniform higher bounds gives convergence in every fixed Sobolev order for smooth data. Passing to the projected equation constructs the solution and its continuous time derivatives. The same difference estimate proves uniqueness. The pressure gradient is the ordinary L^2 gradient projection of $-u \cdot \nabla u$.

Let U_B be the solution with initial datum (5.1), and write X_B for its particle map. The velocity U_B has uniform factorial bounds on a fixed short interval. To see this with the precise factorial convention used earlier, put

$$X_\rho = \sum_{r\ge 0} \frac{\rho^r}{(r!)^2} \sum_{|I|=r} \|\partial^I U_B\|_{H^s}, \qquad Y_\rho = \sum_{r\ge 0} \frac{r\rho^r}{(r!)^2} \sum_{|I|=r} \|\partial^I U_B\|_{H^s}, \qquad s = 6.$$

The factorial product estimates and the preceding transport cancellation give, at each finite truncation of these sums,

$$X_\rho' \le CX_\rho^2 + \left(\frac{\rho'}{\rho} + \frac{CX_\rho}{\rho}\right) Y_\rho.$$

A fixed negative choice of ρ' and a sufficiently short uniform interval keep X_ρ bounded and ρ positive. At a smaller radius, the projected equation bounds $U_{B,t}$ and the material acceleration. Applying the flow composition argument based on (3.55) gives the same kind of factorial bounds for $X_B - \mathrm{id}$, $X_{B,t}$, and $X_{B,tt}$, with a fixed constant K_h. In particular the velocity gradient M_B and pressure Hessian H_B are uniformly bounded. Fix K_B with

$$\lambda_{\max}(H_B(t,x)) \le K_B$$

on this interval. The later choice of time widths will place every construction inside this uniform base interval.

5.2. **The order of choices.** We first fix the constants in Propositions 3.1 and 4.1, then choose the scales for each stage. We use $J-2$ for the base flow, $J-1$ for the first packet, and $j \ge J$ for the subsequent amplification stages, called normal stages below. The integer J is chosen below. Write h_i for the prescribed shear size at stage i, and r for the initial core radius. Their values will be specified after the fixed constants. First choose C_M larger than the absolute target-size constant in the geometric estimates and the base-flow bounds. Choose C_H sufficiently larger than C_M times that target-size constant and the base Hessian bound. These constants will be used in

$$\|M_i\|_{L^\infty} \le C_M h_i, \qquad \|H_i\|_{L^\infty} \le C_H h_i h_{i-1} \quad (i \ge J-1), \qquad h_{J-2} = 1. \tag{5.3}$$

The smallness thresholds in the geometric estimates may depend on these constants; their target-size ratio remains absolute once those thresholds hold. The endpoint quadratic-form estimate in Section 4.2 uses the history bounds with constants C_M, C_H. Fix its constant and then ζ in (4.7), as in that argument.

We reserve the upper Hessian bound $K_B + 1$. Choose an exterior initial bound B_e larger by one than the uniform base bound. In terms of the first shear h_{J-1}, whose value will be fixed by the eventual choice of x_0, define

$$B_c = C_M h_{J-1} + 2, \qquad L = C_1 B_c + 1. \tag{5.4}$$

Here C_1 is the constant in the packet coercivity condition. These formulas define B_c and L as functions of the scale still to be chosen. They are included in polynomial size estimates; they are not uniform bounds as x_0 varies. The bounds maintained throughout the construction are

$$\lambda_{\max}(H_i(t,x)) \le K_B + 1, \qquad \frac{M_i(0,x) + M_i(0,x)^T}{2} \ge \begin{cases} -B_c I, & |x| < r, \\ -B_e I, & |x| \ge r. \end{cases} \tag{5.5}$$

Take the packet hypothesis exponent c_0 larger than the finitely many exponents in the geometric and parent-multiplier estimates. This fixes a finite Q in (3.12). The constants ϑ and C_* are fixed by (3.12) and (3.16), respectively. Let

$$D_0 = 1000,$$

and choose a fixed frequency exponent D_k sufficiently large compared with $(D_0 + 20)Q/\vartheta$ and 1000. Next choose an integer J sufficiently large compared with Q/ϑ, $C_* Q/\vartheta$, the squares of the fixed neighbor-estimate exponents times C_*^2, and the fixed exponents divided by the amplification constant b in (4.12). Increasing J by a fixed factor is allowed. Finally choose x_0 sufficiently large depending on all these choices. The first shear and the bounds B_c, L are then evaluated from their defining formulas; they do not determine new frequency or packet exponents.

The packet exponent is fixed before J, and every first-stage polynomial loss is absorbed by choosing x_0 last.

5.3. **The scale sequence.** The first packet over the base flow prepares the parent for stage J. For $j \ge J$, the time t_{j-1} is the activation time, t_j is the new packet's target time, and S_j is the horizon retained for the next stage. The first amplification stage $j = J$ has activation time zero; all stages $j > J$ have a positive history interval. Define

$$\begin{gathered} x_{J-1} = x_0, \qquad x_j = j^2 x_{j-1} \quad (j \ge J), \\ h_{J-1} = x_0^{D_0}, \qquad k_{J-1} = x_0^{D_k}, \\ r = \ell_{J-1} = x_0^{-D_0}, \qquad \delta_{J-1} = x_0^{-(D_0+10)}, \\ \log h_j = \frac{x_{j-1}}{j^5}, \qquad \log k_j = \frac{x_{j-1}}{j^2}, \\ \log \delta_j^{-1} = \frac{x_{j-1}}{j^3}, \qquad \log \ell_j^{-1} = \frac{x_{j-1}}{j^{7/2}} \quad (j \ge J). \end{gathered} \tag{5.6}$$

Real frequencies k_j are admissible because the periodic angle profile is restricted to a graph on $\mathbb{R}^3$; spatial periodicity is not imposed. Define the available time widths by

$$W_j = \frac{3 x_j x_{j-1}}{\sqrt{h_{j-1}}}, \qquad S_{\text{base}} = 2W_J = 6J^2 x_0^{2 - D_0/2}. \tag{5.7}$$

Set $U^{J-2} = U_B$, $t_{J-1} = 0$, and $S_{J-1} = S_{\text{base}}$. We first construct U^{J-1} on this interval. Subsequently U^j will be constructed on $[0, S_j]$, where its predecessor exists at least until $S_{j-1} = t_{j-1} + 2W_j$.

At stage $j \geq J$, use the geometric parameters a, β from (4.4) at activation $t_0 = t_{j-1}$, with $h_* = h_{j-1}$, $x_{\mathrm{prev}} = x_{j-1}$, and $x_{\mathrm{tar}} = x_j$. Set

$$t_j = t_{j-1} + \frac{x_j}{\sqrt{\beta a h_{j-1}}}, \qquad S_j = t_j + 2W_{j+1}. \tag{5.8}$$

As long as $a, \beta x_{j-1}^2 \in [1/2, 2]$, this gives

$$\frac{W_j}{6} \leq t_j - t_{j-1} \leq \frac{2W_j}{3}. \tag{5.9}$$

5.4. **The estimates maintained at each stage.** At stage $j \geq J$, the packet is built over U^{j-1}, whose primary shear is measured relative to the older solution U^{j-2}. Both solutions therefore enter the induction hypothesis, which consists of the following bounds.

(i) **Parent shear and frame.** The parent U^{j-1} and older solution U^{j-2} are smooth, odd, exact Euler solutions on the common interval $[0, S_{j-1}]$. At the origin on $[t_{j-1}, S_{j-1}]$, the parent has the form (4.3), with older field $B = M_{j-2}$, error $|E| \leq k_{j-1}^{-1/4}$, and $h(t_{j-1}) = h_{j-1}$. The normalized frame evolves according to (4.2).

(ii) **Activation conditions.** At activation, $a, \beta x_{j-1}^2 \in [1/2, 2]$. For $j > J$, the activation inequalities (4.7) also hold. The first stage $j = J$ instead uses the zero-time prescription in Proposition 4.1.

(iii) **Gradient and pressure bounds.** The constructed solutions satisfy the low bounds (5.3) and the one-sided Hessian and initial gradient bounds (5.5) on their respective intervals. The base solution $U^{J-2} = U_B$ has the uniform bounds established above. For $j > J$, the parent's bounds on $[0, t_{j-1}]$, together with $t_{j-1}^{-1} \leq h_{j-1}$, give (4.6).

(iv) **Particle-map bounds.** Both preceding particle maps have the physical factorial bounds (3.16), restricted to the common interval; for the base map we use its uniform constant K_h. For the current parent we use $K_h = k_{j-1}^{C_*}$, and at positive-history stages require $t_{j-1}^{-1} \leq K_h^c$.

The first-packet construction below establishes this state for $j = J$. The inductive step constructs U^j on $[0, S_j]$ and establishes the same state for $j + 1$. We first check the scale inequalities used in both steps.

5.5. **Verifying the scale requirements.** As the parent shear grows, its coefficient bounds also grow. The packet construction remains applicable provided the new frequency dominates them in the sense of (3.12). Expressing those bounds in terms of the chosen scales makes this condition explicit.

Packet smallness. At a normal stage, let P_j be a sufficiently large fixed constant plus fixed multiples of

$$k_{j-1}^{C_*}, \quad \ell_j^{-1}, \quad \delta_j^{-1}, \quad h_j, \quad h_{j-1}, \quad h_{J-1}, \quad r^{-1}, \quad S_{\mathrm{base}}^{-1}, \quad x_j, \quad x_{j-1}. \tag{5.10}$$

The first entry is the physical parent bound K_h. We may take $\Theta = C(1 + x_j x_{j-1})$, and $\varepsilon^{-1} \leq C\sqrt{h_{j-1}} \leq C h_{j-1}$. For $j > J$, the recursion for x_j gives the exact identities

$$\log k_{j-1} = \frac{x_{j-1}}{(j-1)^4}, \qquad \log h_{j-1} = \frac{x_{j-1}}{(j-1)^7}. \tag{5.11}$$

Consequently, for a fixed C' also covering the first-stage power D_k,

$$\frac{\log P_j}{\log k_j} \leq C \left\{ \frac{1}{j} + \frac{C_*}{j^2} + \frac{j^2 \left(\log x_{j-1} + C' \log x_0 + C' \log J\right)}{x_{j-1}} \right\}. \tag{5.12}$$

Choose J and then x_0 so that the right side is less than $\vartheta/(100Q)$. Thus $P_j^Q \leq k_j^{\vartheta/100}$ at every stage. The same ratio tends to zero as $j \to \infty$. Uniformity follows directly from $x_j = j^2 x_{j-1}$: for each fixed A, the quantities $j^A \log x_{j-1}/x_{j-1}$ decrease at least geometrically once J and x_0 are sufficiently large. At the first packet stage the parent bound is fixed, and we may take $P_{J-1} \leq C(J) x_0^{D_0+20}$ without including k_{J-1}; the choice of D_k proves the required smallness there. Thus the packet condition (3.12) holds at the seed and every normal stage.

Compatible time intervals. The widths satisfy

$$\frac{W_{j+1}}{W_j} = j^2 (j+1)^2 \sqrt{\frac{h_{j-1}}{h_j}}.$$

For $j > J$, the logarithm of the square-root factor is

$$-\frac{x_{j-1}}{2j^5} + \frac{x_{j-1}}{2(j-1)^7}.$$

For $j = J$ the second term is instead $(D_0/2) \log x_0$. In both cases the negative term dominates all logarithmic factors. In particular, the horizons nest, $S_j \leq S_{j-1}$, and the extra scaled time after target satisfies

$$2\sqrt{a h_{j-1}}\, W_{j+1} \leq \Theta^{-60}. \tag{5.13}$$

Also $t_J \geq S_{\text{base}}/12$. At positive-history stages, $t_0^{-1} \leq h_{j-1} \leq K_h^c$. Every inverse horizon occurring in a packet solve is polynomially bounded: either $S = S_{\text{base}}$ or $S \geq t_J$.

Geometric stability and shear separation. The error in (4.5) has three contributions: variation of the older field, the inherited packet error, and variation across the new packet support. Take

$$E_* = k_{j-1}^{-1/4}, \qquad G_* = 1 + h_{j-2}.$$

At $j = J$, we have $G_* = 2$, $\varepsilon \leq C x_0^{-500}$, and $\Theta \leq C J^2 x_0^2$. Therefore

$$\varepsilon \Theta^{61} G_*^2 \ll x_0^{-10}.$$

The preceding packet error has arbitrarily strong polynomial decay by the choice of D_k, and the variation across packet labels, represented by $\ell_j K_h^c/\varepsilon$ in (4.5), includes $\exp(-x_0/J^{7/2})$, which dominates all fixed powers of x_0. At $j = J+1$, the older size is $G_* = 1 + x_0^{D_0}$, while $\log \varepsilon = -x_0/(2J^5) + O(1)$. At subsequent stages,

$$\begin{aligned}
\log(\varepsilon G_*^2) &\leq -\frac{x_{j-1}}{2(j-1)^7} + \frac{2x_{j-1}}{(j-1)^2 (j-2)^7} + C \\
&\leq -\frac{2x_{j-1}}{5(j-1)^7} + C.
\end{aligned}$$

This dominates every fixed power of Θ and x_{j-1}. The contribution from variation across packet labels has logarithm at most

$$-\frac{x_{j-1}}{j^{7/2}} + \frac{c C_* x_{j-1}}{(j-1)^4} + \frac{C x_{j-1}}{(j-1)^7} + C.$$

Our choice of J makes this at most $-x_{j-1}/(2j^{7/2})$. Finally, the preceding frequency error has logarithm $-x_{j-1}/(4(j-1)^4)$. These comparisons prove (4.5), with any fixed enlargement of its constants. The additional requirements $\beta \le \beta_0$ and $x_{\mathrm{tar}} \ge 2$ hold because $\beta \le 2x_{j-1}^{-2}$ and $x_j \ge J^2 x_0$. They also prove

$$h_j \gg h_{j-1}^2, \qquad \frac{\sqrt{h_{j-1}}}{x_{j-1}x_j} \gg G_* + 1, \qquad \ell_j < r, \tag{5.14}$$

including the first and second normal stages.

Summable pressure and history costs. To preserve the upper Hessian and initial gradient bounds (5.5), we sum the increments in Claim 1 of Proposition 3.1. On the history interval and where $\tau < 1$, the size ratio (4.12), the normalization (4.13), and the parent bound (5.3) bound both leading increments by

$$b_j = C h_j h_{j-1} K_h^c \Theta^c \varepsilon^{-c} e^{-b x_{j-1}}. \tag{5.15}$$

For $j > J$, the logarithm of the prefactor $C h_j h_{j-1} K_h^c \Theta^c \varepsilon^{-c}$ is bounded by $C(c, C_*) x_{j-1}/(j-1)^4 + C \log(x_j h_{J-1})$. Increasing J and then x_0 gives $b_j \le e^{-b x_{j-1}/2}$; the first stage obeys the same conclusion with a possibly smaller fixed exponent.

On $\tau \ge 1$, the sign (4.9) and the lower bound $f_\delta' \ge -C$ in (3.4) control the positive part of the pressure-Hessian increment (3.14). The normalization (4.13) and the size comparison in Claim 3 of Proposition 4.1 bound this cost by $C\delta_j h_j h_{j-1}$. The scales (5.6) give

$$\delta_j h_j h_{j-1} \le \exp\left(-\frac{x_{j-1}}{2j^3}\right). \tag{5.16}$$

The remaining errors are the $k_j^{-1/4}$ remainders in (3.13) and (3.14). The sums of these quantities, and the sums of x_{j-1}^{-c} for every fixed $c > 0$ used below, can be made as small as prescribed by choosing x_0 last. Indeed each positive exponent x_{j-1}/j^A in these decay estimates grows at least geometrically after J. The seed cost is also small: $\delta_{J-1} h_{J-1} = x_0^{-10}$.

Coercivity. Finally, $S_{\mathrm{base}} \to 0$ and $h_{J-1} r^3 S_{\mathrm{base}} \to 0$. Hence, with a strict margin,

$$\frac{(K_B+1)S^2}{2} + B_e S + C_2 B_c r^3 S \le \frac{1}{2} \qquad (0 < S \le S_{\mathrm{base}}). \tag{5.17}$$

This verifies the time and initial-data part of (3.11). None of these comparisons requires an inequality of the form $e^{P_j^c} \ll k_j$.

5.6. **The first packet.** We construct U^{J-1} over $U^{J-2} = U_B$. This seed packet supplies the parent shear and frame required by Section 5.4 for the first amplification stage $j = J$. Apply Proposition 3.1 over U_B on $[0, S_{\mathrm{base}}]$ with

$$\ell = \ell_{J-1}, \quad k = k_{J-1}, \quad \delta = \delta_{J-1}, \quad m_0 = p, \quad v(0) = q, \quad \alpha = \delta_{J-1} h_{J-1}, \quad L = 0.$$

For this application the base initial bound holds everywhere, so we use the coercivity condition with $B_c = 0$. The homogeneous propagator is bounded on this short interval, and we may take $g = 1$. On the packet support, $m \cdot M_B v = 1$ initially. Along a base particle, $\dot{M}_B = -M_B^2 - H_B$; the base bounds and the ray and velocity equations therefore give

$$m \cdot M_B v \ge \frac{1}{2} \quad \text{on } [0, S_{\mathrm{base}}].$$

The packet hypotheses hold, and we obtain a smooth odd solution U^{J-1}. The output expansions yield

$$\|M_{J-1}\|_\infty \le C_M h_{J-1}, \qquad \|H_{J-1}\|_\infty \le C_H h_{J-1}.$$

Because the leading Hessian increment is a negative multiple of $m \otimes m$ where $f'_\delta \ge 0$, and $f'_\delta \ge -C$ everywhere, its upper-eigenvalue cost is at most

$$C\delta_{J-1}h_{J-1} + k_{J-1}^{-1/4}.$$

At time zero, the mean coefficients $B_p(0)$ and the forced oscillatory coefficients $A_p(0), C_p(0)$ with $p \ge 2$ vanish. Thus the initial exterior bound outside $|x| < r$ is unchanged; inside that ball, $B_c = C_M h_{J-1} + 2$ leaves a strict margin.

At the fixed origin, the packet expansion gives

$$M_{J-1} = M_B + h(t)q(t)p(t)^T + E(t), \qquad |E(t)| \le k_{J-1}^{-1/4}, \qquad h(t) = \frac{\alpha|m(t)||v(t)|}{\delta_{J-1}}.$$

The normalized ray and velocity form the orthonormal pair $p(t), q(t)$, and $h(0) = h_{J-1}$. Their equations give $h'/h = -(M_B)_{pp} - (M_B)_{qq}$. At activation $t_0 = 0$, the prescribed base matrix gives exactly

$$a = 1, \qquad \beta = x_0^{-2}.$$

There is no positive-history endpoint condition at stage $j = J$, since its activation time is $t_{J-1} = 0$. The physical flow bound (3.16) supplies $K_h = k_{J-1}^{C_*}$ for the next packet. Together with the base-flow bounds, these estimates establish the state in Section 5.4 for $j = J$.

5.7. **The inductive step.** Assume the bounds in Section 5.4 at stage $j \ge J$. We construct U^j on $[0, S_j]$ with central target gradient

$$M_j(t_j, 0) = M_{j-1}(t_j, 0) + h_j q_2 p_2^T + O(k_j^{-1/4}),$$

where $p_2 = m(t_j, 0)/|m(t_j, 0)|$ and $q_2 = v(t_j, 0)/|v(t_j, 0)|$ are the new frame in Claim 2 of Proposition 4.1. The normalization (4.13) and Claim 1 of Proposition 3.1 give this gradient. We then verify the bounds of Section 5.4 for $j+1$: the summed costs from §5.5 preserve (5.5), the estimates (4.10) and (4.11) give the next activation parameters, and (3.16) controls the new particle map.

Constructing the child solution. Write $B = M_{j-2}$ for the older field at the origin. The origin is fixed by oddness. The gradient equation there gives

$$\dot{B} = -B^2 - H_{j-2}, \qquad \|B\| \le CG_*, \qquad \|\dot{B}\| \le CG_*^2, \qquad G_* = 1 + h_{j-2}.$$

For $j = J$, the same assertions use the uniform base bounds. Define t_j, S_j by (5.8) and restrict the parent to $[0, S_j]$. If $j > J$, choose the transverse endpoint data as in (4.8); if $j = J$, use $v(0) = q$. The scale checks verify all geometric hypotheses. Normalize the wave by

$$\alpha_j = \frac{\delta_j h_j}{|m(t_j, 0)||v(t_j, 0)|}. \tag{5.18}$$

Use ℓ_j, k_j, δ_j and the boundary parameter $L = C_1 B_c + 1$ in the packet construction. The preceding physical flow estimates imply the required multiplier bounds: differentiation, cofactor inversion of the volume-preserving flow matrix, and factorial products cost fixed powers of the parameter K_h. Coercivity follows from (5.17). The geometric estimates give the transverse propagator bound, the bound on $\alpha_j g$, and

$$\alpha_j \le P_j^c e^{-bx_{j-1}}.$$

We have therefore constructed an exact smooth odd Euler solution U^j on $[0, S_j]$, with physical flow bound (3.16) at frequency k_j.

Preserving the global and initial bounds. We next verify the bounds Equations (5.3) and (5.5) needed to continue the induction. On the interval $\tau \geq 1$, the absolute target-size comparison and the packet output give

$$\|M_j - M_{j-1}\|_\infty \leq Ch_j + k_j^{-1/4},$$
$$\|H_j - H_{j-1}\|_\infty \leq CC_M h_j h_{j-1} + k_j^{-1/4}.$$

The sign $m \cdot M_{j-1}v > 0$, the nonnegative cutoff χ_1, and $f'_{\delta_j} \geq -C$ give the sharper upper-eigenvalue increment

$$\lambda_{\max}(H_j) \leq \lambda_{\max}(H_{j-1}) + CC_M\delta_j h_j h_{j-1} + k_j^{-1/4}.$$

Outside the leading packet support its leading term is zero. On the history interval and where $\tau < 1$, both absolute increments are bounded by $C(1 + C_M)b_j + k_j^{-1/4}$. The summed positive costs, including the seed, are less than the reserved unit of slack, so

$$\lambda_{\max}(H_j) \leq K_B + 1.$$

The absolute bounds (5.3) follow from the choices of C_M, C_H and $h_j \gg h_{j-1}^2$. At time zero, every normal-stage increment is bounded by the summable cost (5.15); this includes $j = J$, for which $t_0 = \tau = 0$. The initial exterior and core bounds persist with a strict margin. These statements use the exact pressure expansion (3.14); no spatial locality of the pressure is assumed.

Transferring the primary frame and activation conditions. Finally consider the new primary frame at the origin. On $[t_j, S_j]$, parity keeps the graph angle equal to zero, so the child gradient M_j has the form

$$M_j = M_{j-1} + h(t)q_2(t)p_2(t)^T + E_j(t), \qquad |E_j| \leq k_j^{-1/4},$$
$$h(t) = \frac{\alpha_j |m(t)||v(t)|}{\delta_j}, \quad h(t_j) = h_j.$$

The new frame evolves over the older field M_{j-1}, and $h'/h = -(M_{j-1})_{p_2p_2} - (M_{j-1})_{q_2q_2}$. The parameter-transfer formula (4.10) shows that the relative errors in successive values of a are absolutely summable: they are bounded by a fixed multiple of

$$x_j^{-4} + \frac{\beta}{x_j^2} + \frac{\sqrt{\beta}}{x_j^3} + e_*\Theta^{40}.$$

Their sum can be made arbitrarily small. Starting from $a = 1$, their product therefore stays in $[1/2, 2]$. The other transfer estimate gives directly $\beta_{\text{new}} x_j^2 \in [1/2, 2]$; these errors need not be multiplied across stages.

The compression estimate and (5.14) give

$$p_2 \cdot M_{j-1}p_2 \leq -\frac{c\sqrt{h_{j-1}}}{x_{j-1}x_j} + C(G_* + E_*) < -1.$$

Adding E_j preserves strict negativity, while

$$\frac{\|M_{j-1} + E_j\|}{h_j} \leq \frac{C_M h_{j-1} + 1}{h_j} < \zeta.$$

Thus (4.7) holds at the next activation. The bounds on $[0,t_j]$ and $t_j^{-1} \le h_j$ give the required positive-history hypotheses there. Every part of Section 5.4 now holds with j replaced by $j+1$, closing the induction.

6. The limiting initial datum and finite-time breakdown

Although $|\nabla U^j(t_j,0)|$ tends to infinity, these gradients belong to solutions with different initial data. To prove Theorem 1.1, we must construct an initial datum u_0 whose solution breaks down. First, Section 6.1 uses the initial increment estimates to obtain convergence in every fixed Sobolev norm. Next, Section 6.2 shows that a smooth solution from the limiting datum persisting past the accumulation time would inherit the growing gradients by stability. Finally, Section 6.3 proves that $\|\nabla u(t)\|_\infty$ is unbounded as $t \uparrow T_*(u_0)$ and that $\int_0^{T_*(u_0)} \|\operatorname{curl} u(t)\|_\infty \, dt = \infty$.

6.1. **Smooth convergence at the initial time.** At stage j, split $U^j(0) - U^{j-1}(0)$ into the oscillatory and mean increments defined in (3.59). For every fixed integer m, their H^m norms satisfy (3.17). Since $\alpha_j \le P_j^c e^{-bx_{j-1}}$ and $\log P_j = o(\log k_j)$, the logarithms of their H^m norms are bounded respectively by

$$-bx_{j-1} + \frac{mx_{j-1}}{j^2} + \frac{mx_{j-1}}{j^{7/2}} + C_m \log P_j, \tag{6.1}$$

$$-\frac{2x_{j-1}}{j^2} + \frac{mx_{j-1}}{j^{7/2}} + C_m \log P_j. \tag{6.2}$$

For sufficiently large j depending on m, these are at most $-bx_{j-1}/2$ and $-x_{j-1}/j^2$, respectively. Both exponentials are summable. The mean increment $u_{\text{mean},0}$ is independent of θ, so differentiating it does not produce the phase factor k_j^m. This gives the stronger decay in (6.2).

The sequence $U^j(0)$ is therefore Cauchy in every H^m. All initial high increments are supported in $|a| \le \ell_j/2$, and the compact boundary operator confines all initial means to $|a| \le 2$. Together with the fixed base support, these lie in one fixed ball. The limit

$$u_0 = \lim_{j\to\infty} U^j(0) \quad \text{in every } H^m(\mathbb{R}^3) \tag{6.3}$$

is consequently smooth, compactly supported, odd, and divergence-free.

6.2. **Non-persistence of the smooth solution.** The times t_j in (5.8) increase and are bounded by S_{base}, as verified in §5.5. Consequently their accumulation time

$$T_\infty = \lim_{j\to\infty} t_j \quad \text{satisfies} \quad 0 < t_J \le T_\infty \le S_{\text{base}}. \tag{6.4}$$

Let u be the maximal smooth Euler solution with initial datum u_0. Local existence gives $T_*(u_0) > 0$. Suppose, for contradiction, that $T_*(u_0) > T_\infty$. Then all Sobolev norms of u are bounded on $[0, T_\infty]$. Compare U^j with u on $[0,t_j]$, where U^j exists, and write $w = U^j - u$. Its equation is

$$\partial_t w + u\cdot\nabla w + w\cdot\nabla u + w\cdot\nabla w + \nabla(p_j - p) = 0, \qquad \operatorname{div} w = 0.$$

Since $\operatorname{div}(u+w) = 0$, each derivative word I satisfies $\langle \partial^I w, (u+w)\cdot\nabla\partial^I w\rangle_{L^2} = 0$. The remaining H^3 commutators and the product $w\cdot\nabla u$ give

$$y'(t) \le C_u y(t) + C y(t)^2, \qquad y(t) = \|w(t)\|_{H^3}, \tag{6.5}$$

where C_u depends on $\sup_{[0,T_\infty]} \|u\|_{H^4}$ and is independent of j. For example, while $y \le 1$, $y(t) \le y(0)e^{(C_u+C)T_\infty}$. Since $y(0) \to 0$, this bootstrap closes for all sufficiently large j, proving

$$\sup_{0\le t\le t_j} \|U^j(t) - u(t)\|_{H^3} \longrightarrow 0.$$

On the other hand the primary expansion at the target gives

$$\|M_j(t_j,0)\| \ge h_j - C_M h_{j-1} - k_j^{-1/4} \longrightarrow \infty.$$

This contradicts $H^3 \hookrightarrow C_b^1$ and the preceding convergence. Hence

$$0 < T_*(u_0) \le T_\infty \le S_{\text{base}} < \infty. \tag{6.6}$$

The maximal lifespan may end before T_∞; this upper bound is sufficient for finite-time breakdown. The comparison on the intervals $[0,t_j]$ was made under the contradiction assumption $T_*(u_0) > T_\infty$.

6.3. **Continuation criteria at the endpoint.** Set $T = T_*(u_0) < \infty$. We now prove the two divergence assertions of Theorem 1.1: the velocity gradient satisfies $\limsup_{t\uparrow T} \|\nabla u(t)\|_\infty = \infty$, and the vorticity satisfies $\int_0^T \|\operatorname{curl} u(t)\|_\infty \, dt = \infty$.

Suppose, for contradiction, that $B := \sup_{0\le t<T} \|\nabla u(t)\|_\infty < \infty$. By (5.2),

$$\sup_{0\le t<T} \|u(t)\|_{H^3} \le \|u_0\|_{H^3} e^{C_3BT} \le M_3 := \max\{1, \|u_0\|_{H^3} e^{C_3BT}\}.$$

The local theory in Section 5.1 supplies a time $\delta_0 = \delta_0(M_3) > 0$, uniform for smooth divergence-free data of H^3 norm at most M_3. For each $s \in [0,T)$, let v_s be the solution starting from $v_s(s) = u(s)$ on $[s, s+\delta_0)$. Fix an embedding constant $C_{\text{emb}} > 0$ such that $\|\nabla f\|_\infty \le C_{\text{emb}} \|f\|_{H^3}$, and set

$$\delta = \min\left\{\frac{\delta_0}{2}, \frac{1}{2C_3 C_{\text{emb}} M_3}\right\} > 0.$$

The energy inequality at order three gives

$$\|v_s(t)\|_{H^3} \le \frac{M_3}{1 - C_3 C_{\text{emb}} M_3 (t-s)} \le 2M_3 \qquad (s \le t \le s+\delta).$$

For every integer $m \ge 3$, the same inequality before and after the restart yields, on this common interval,

$$\|v_s(t)\|_{H^m} \le \|u(s)\|_{H^m} e^{2C_m C_{\text{emb}} M_3 \delta} \le \|u_0\|_{H^m} e^{C_m BT + 2C_m C_{\text{emb}} M_3 \delta}.$$

Thus all higher Sobolev norms remain finite on the interval of length δ, which does not depend on m or s. Choose $s \in (\max\{0, T-\delta/2\}, T)$. Uniqueness gives $v_s = u$ on $[s,T)$, while $s + \delta > T$, so v_s gives a smooth extension past T. This contradicts maximality. Since u is smooth on every compact subinterval of $[0,T)$, a finite limsup of $\|\nabla u(t)\|_\infty$ at T would make B finite. It follows that

$$\limsup_{t\uparrow T_*(u_0)} \|\nabla u(t)\|_\infty = \infty.$$

We also give the vorticity formulation. Write $\omega = \operatorname{curl} u$. The whole-space Biot–Savart identity is $u = \operatorname{curl}(-\Delta)^{-1}\omega$. Thus ∇u is a constant local matrix applied to ω, plus a principal-value integral whose kernel K has degree -3, smooth angular dependence, and zero spherical mean. For $0 < d < 1/2$, split this integral into $|z| < d$, $d < |z| < 2$, and a smoothly cut off far region. On the inner region, subtract $\omega(x)$ and use $H^3 \hookrightarrow C^{1,\lambda}$, $0 < \lambda < 1/2$, to get

$$\left| \int_{|z|<d} K(z)[\omega(x-z) - \omega(x)]\, dz \right| \le C d^{\lambda} \|u\|_{H^3}.$$

The middle region contributes $C\|\omega\|_\infty \log(2/d)$. On the far region, integrate $\omega = \operatorname{curl} u$ onto the cut-off kernel; its differentiated kernel belongs to L^2, so this contributes $C\|u\|_2$. Choosing $d = c(e + \|u\|_{H^3})^{-1/\lambda}$ and using conservation of kinetic energy gives

$$\|\nabla u\|_\infty \le C\left[1 + \|u_0\|_2 + \|\omega\|_\infty \log(e + \|u\|_{H^3})\right]. \tag{6.7}$$

With $Z = \log(e + \|u\|_{H^3})$, (5.2) implies

$$Z' \le C(1 + \|u_0\|_2) + C\|\omega\|_\infty Z.$$

If $\int_0^{T_*} \|\omega(t)\|_\infty\, dt$ were finite, Gronwall's inequality would bound Z, hence $\sup_{t<T} \|u(t)\|_{H^3}$. The embedding $H^3 \hookrightarrow C^1$ and the preceding restart argument would then extend u past T, contradicting maximality. Therefore the datum (6.3) satisfies

$$\int_0^{T_*(u_0)} \|\omega(t)\|_{L^\infty(\mathbb{R}^3)}\, dt = \infty.$$

The datum in (6.3), the finite lifespan in (6.6), and the two continuation conclusions above prove Theorem 1.1.

References

1. J. Thomas Beale, Tosio Kato, and Andrew Majda, *Remarks on the breakdown of smooth solutions for the 3-D Euler equations*, Communications in Mathematical Physics **94** (1984), no. 1, 61–66, https://doi.org/10.1007/BF01212349.
2. Jiajie Chen, *Asymptotically self-similar blowup for 3D incompressible Euler with $C^{1,1/3-}$ velocity II: 3D profiles, blowup, and limiting behavior*, arXiv:2605.15130, 2026, https://arxiv.org/abs/2605.15130.
3. Jiajie Chen and Thomas Y. Hou, *Stable nearly self-similar blowup of the 2D Boussinesq and 3D Euler equations with smooth data I: Analysis*, arXiv:2210.07191, 2022, https://arxiv.org/abs/2210.07191.
4. ______, *Stable nearly self-similar blowup of the 2D Boussinesq and 3D Euler equations with smooth data II: Rigorous numerics*, Multiscale Modeling & Simulation **23** (2025), no. 1, 25–130, https://doi.org/10.1137/23M1580395.
5. Diego Córdoba, Luis Martínez-Zoroa, and Fan Zheng, *Finite time singularities to the 3D incompressible Euler equations for solutions in $C^\infty(\mathbb{R}^3 \setminus \{0\}) \cap C^{1,\alpha} \cap L^2$*, Annals of PDE **11** (2025), 19, https://doi.org/10.1007/s40818-025-00214-2.
6. Tarek M. Elgindi, *Finite-time singularity formation for $C^{1,\alpha}$ solutions to the incompressible Euler equations on $\mathbb{R}^3$*, Annals of Mathematics **194** (2021), no. 3, 647–727, https://doi.org/10.4007/annals.2021.194.3.2.
7. Tarek M. Elgindi, Tej-Eddine Ghoul, and Nader Masmoudi, *On the stability of self-similar blow-up for $C^{1,\alpha}$ solutions to the incompressible Euler equations on $\mathbb{R}^3$*, Cambridge Journal of Mathematics **9** (2021), no. 4, 1035–1075, https://arxiv.org/abs/1910.14071.
8. Tarek M. Elgindi and Federico Pasqualotto, *From instability to singularity formation in incompressible fluids*, arXiv:2310.19780, 2023, https://arxiv.org/abs/2310.19780.
9. Susan Friedlander and Misha M. Vishik, *Instability criteria for the flow of an inviscid incompressible fluid*, Physical Review Letters **66** (1991), no. 17, 2204–2206, https://doi.org/10.1103/PhysRevLett.66.2204.
10. Tosio Kato, *Nonstationary flows of viscous and ideal fluids in R^3*, Journal of Functional Analysis **9** (1972), no. 3, 296–305, https://doi.org/10.1016/0022-1236(72)90003-1.
11. Alexander Lifschitz and Eliezer Hameiri, *Local stability conditions in fluid dynamics*, Physics of Fluids A **3** (1991), no. 11, 2644–2651, https://doi.org/10.1063/1.858153.
12. Steve Shkoller, *Incompressible Euler blowup at the $C^{1,1/3}$ threshold*, arXiv:2603.10945, 2026, https://arxiv.org/abs/2603.10945.